The accelerator complex at Serpukhov (IHEP)

S. A. Chernyĭ
Institute of High Energy Physics, Serpukhov

Fiz. Elem. Chastits At. Yadra **22**, 1067–1128 (September–October 1991)

The systems of the accelerator complex of the IHEP at Serpukhov are described, and their technical characteristics are presented.

INTRODUCTION

The accelerator complex at IHEP is the largest base in the country for investigations in the field of high-energy physics. The development and improvement of such complexes is a necessary condition for the development of a dynamical branch of physics like the study of elementary particles. The idea of developing a new accelerator center was put forward in the middle of the fifties. It was proposed that the accelerator complex should be designed for an energy of 50–60 GeV and a proton intensity of $\sim 10^{12}$ particles/cycle and consist of an injector, a linear accelerator to energy 100 MeV, and the main accelerator, a synchrotron. The further development of this question by many scientific and engineering groups in the country culminated in the major project of the accelerator complex at the IHEP. The commissioning of the accelerator in 1967 and the first physics investigations in 1968 marked the beginning of a whole series of scientific studies in high-energy physics. The results of the physics experiments largely determined new directions of development and posed new problems for accelerator topics; on the other hand, the improvement of the accelerator complex opened up new possibilities for physics experiments. Investigations in the field of accelerator technology made it possible to pose the problem of increasing the beam intensity from that of the original project by 50 times. The accelerator complex has in the meanwhile been modernized to a considerable extent, and changes have occurred not only in the basic facility but also in the systems that form the complex. This has included the development and construction of a new injector for the main accelerator—a rapid-cycling ring accelerator, for which, in its turn, the injector is a new linear accelerator. A developed system of particle channels has been designed and constructed; it ensures beams of particles with the required parameters for experimental purposes. The corresponding studies have been reflected in numerous publications on individual systems, and also in review papers. However, it has become more and more difficult to get an overall picture of the accelerator complex as it has developed and been modernized, since information about the systems is scattered in publications over a period of two decades. The wish to eliminate this difficulty, at least partly, was the basis of the present paper.

The IHEP accelerator complex consists of a chain of three accelerators: a linear accelerator to energy 30 MeV, a ring injector to energy 1.5 GeV, and the main accelerator U-70 with final working energy 70 GeV of the particles (Fig. 1). The beam extraction systems ES ensure operation of not only internal targets set up in the vacuum chamber of the accelerator but also of external targets, in which, as a rule, more intense beams of secondary particles can be produced than in internal targets. The system of channels forms beams with the required parameters and transports them to the experimental facilities situated in the buildings 1BV, 2 and 2A, PK-1, PK-2.

1. THE LINEAR ACCELERATOR

The proton accelerator URAL-30 [Uskoritel' Rezonansnyĭ Avtofokusiruyushchiĭ Lineĭnyĭ (Accelerator Resonance Autofocusing Linear)] has a particle energy 30 MeV at its exit and a working value of the current up to 100 mA. The accelerating system consists of an ion gun with output energy 100 keV, the initial part of the accelerator, up to energy 2 MeV, two sections of the main part of the accelerator, to 16 and 30 MeV, and a beam debuncher. The operation of the accelerating system is made possible by an rf supply system, the electrical supply, thermostatic control, etc. A block diagram of the accelerator is shown in Fig. 2. Let us consider the basic systems of the accelerator.

Ion gun

The main components of the ion gun (IG), which is of the duoplasmatron type,[1] are the ion source (IS), the ion optics (IO), the energy sources, the control system, and the parameter control (PC). The ion source[2] ensures generation of a hydrogen plasma and consists of three chambers next to each other, so that the anode of the first chamber is the cathode of the second, etc. (Fig. 3). In the anode–cathode electrodes of the chambers there are coaxial cylindrical cavities, by which the discharge chambers of the source are connected to each other. Between the electrodes of the ion source a pulsed voltage up to 2 kV is applied. At a pressure 30–70 Pa of the hydrogen in the first cathode chamber of the ion source an arc discharge is initiated and ensures a directed plasma jet, which is the emitter for the second chamber. The pulsed voltage is applied later to the electrodes of the final, main chamber, when there is already stable burning of the plasma in the intermediate chamber. The main chamber of the source is in a magnetic field, and by varying the strength of this field the output current of the gun can be changed. Through an opening of diameter 1.5 mm in the anode of the source, the hydrogen plasma diffuses into an expander, which is the initial part of the ion optics of the gun.

The ion optics forms a beam by means of the expander and extracting and grounded electrodes. The expander

 0090-4759/91/050520-32$04.00

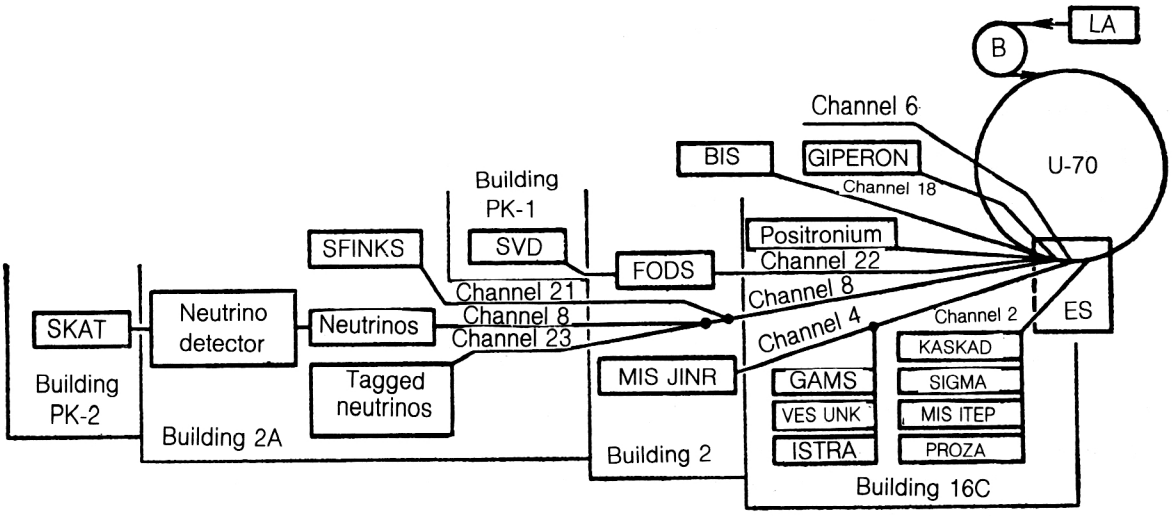

FIG. 1. Schematic arrangement of the IHEP accelerator complex: LA is the linear accelerator to 30 MeV; B is the booster synchrotron to 1.5 GeV; U-70 is the synchrotron to energy 70 GeV; ES are beam extraction systems; GAMS, SKAT, etc., are experimental facilities; Channel denotes a magneto-optical channel for transporting the charged particles.

consists of sections joined by partitions, the gaps between these being used to evacuate the volume of the expander. The final section of the expander, facing the extracting electrode, is insulated from the anode of the ion source and is at the floating potential of the plasma. This construction made it possible to stabilize the plasma and obtain a uniform density. The extracting electrode is in the form of a frustum of a cone, and the grounded electrode is flat. At the center of the electrodes are openings through which the accelerated proton beam can pass. The main accelerating voltage, 100 kV, is applied between the expander and the grounded electrode; the focusing voltage is applied between the extracting and grounded electrodes, so that between the expander and the extracting electrode the voltage is equal to the sum of the main voltage and the focusing voltage. Between the extracting and grounded electrodes, the proton beam is decelerated to the base energy. The advantage of this arrangement is that, for unchanged main voltage and, therefore, unchanged exit energy of the proton beam, it is possible, by varying the voltage on the extracting electrode, to change at the gun output the diameter and divergence of the beam and also other parameters in order to make investigations in the beam.

The ion gun is supplied by several sources, the main ones of which are the modulator of the ion source and the high-voltage source of the ion optics. The modulator is used to produce on the electrodes of the ion source an ignition pulse of voltage ~ 2 kV and is based on a shaping line with scheme to stabilize the charge of the line to accuracy $2\text{–}10^{-3}$. The line is made up of concentrated LC elements. Electronic switches that short the LC line are made of transistors, switching of which results in discharge of the line to the electrodes of the ion source. The current of the cathode chamber is 100–120 A, and that of the intermediate chamber is ~ 100 A with duration 60–70 μsec of the current pulse. The anode current of the main chamber of the source is 70–90 A with pulse duration up to 20 μsec and duration 2–3 μsec of the pulse fronts.

The high-voltage source that produces the voltages on the expander and extracting electrode consists of two identical modulators of pulsed currents feeding two pulsed transformers with transformation coefficient 125. The

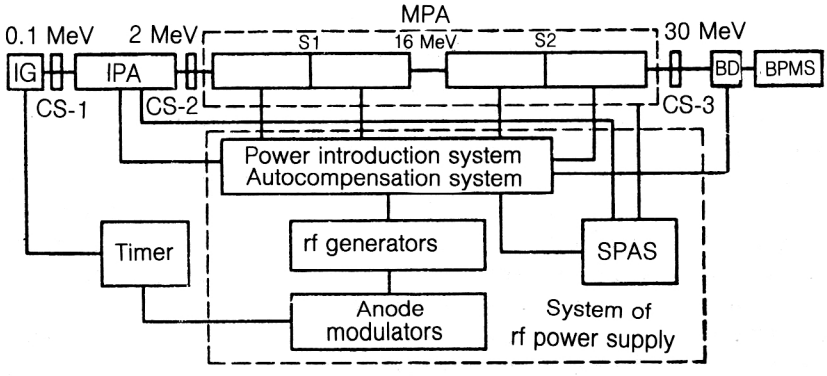

FIG. 2. Structural diagram of the linear accelerator URAL-30: IG is the ion gun; IPA is the initial part of the accelerator, S1 and S2 are sections of the main part of the accelerator (MPA); BD is the beam debuncher; CS are current sensors; BPMS is the beam parameter measuring system; SPAS is the slow phase autoregulation system.

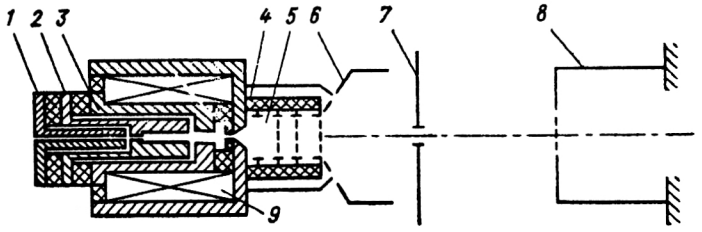

FIG. 3. Schematic arrangement of ion source and ion optics: 1) hollow cathode (molybdenum); 2) anode–cathode; 3) anode–cathode (bimetal); 4) main anode (copper); 5) sectioned expander; 6) controlling electrode; 7) extracting electrode; 8) grounded electrode; 9) magnetic lens.

modulators are fed from charge devices with remote-controlled voltage.

The control system is mounted in a stand, which carries, in addition, the control block of the electromagnetic valve, by means of which hydrogen is supplied to the chambers of the source, the source of the stabilized current of the magnetic lens, the amplifiers, and also the timer synchronized with the systems of the following accelerators.

The parameters of the ion gun are as follows:

Output energy	100 keV
Proton current in working regime	150 mA
Duration of current pulse (working regime)	10 μsec
Stability of current	$\pm 3\%$
Normalized emittance of beam	$0.1\pi \cdot 10^{-5}$ rad·m
Proton component of beam	90–95%

Accelerating system

In the accelerator URAL-30, accelerting systems of two types, which differ from the traditional Alvarez accelerating system, are used. In the section of the initial part of the accelerator there is a structure with electrodes formed by a long four-lead line with spatially homogeneous quadrupole focusing.[3,4] In the sections of the main part of the accelerator, structures with double accelerating gap and focusing rf field are used.[5,6] In both types of structure, the rf field at the electrodes is produced by means of an H resonator.[7–9] These accelerating structures have a number of advantages over the traditional Alvarez–Blewett accelerator, the scheme of which was followed in the injector I-100 (linear accelerator of protons to 100 MeV)[10] previously used with the U-70 accelerator. An accelerator based on the Alvarez–Blewett scheme (cylindrical resonator excited in the wave E_{010} and loaded with drift tubes with quadrupole lenses built into them) requires a high-voltage injector and has a considerable size. The injection energy is determined by the possibility of arranging along the length of a period the structures of quadrupole magnetic lenses in drift tubes, which are shorter, the lower the energy of the accelerated particles. Thus, the construction sizes introduce restrictions on the energy of injection into the accelerator. In addition, the lower injection energy in an Alvarez accelerator leads to larger Coulomb effects, which significantly lower the limiting beam current. An accelerating structure with spatially homogeneous quadrupole focusing opens up new possibilities for lowering the injection energy (to about 100 keV) without significant loss of beam intensity.

Initial part of the accelerator

The accelerating structure is a high-frequency focusing four-lead long line (Fig. 4a), in which the longitudinal accelerating component of the field is produced by periodic modulation of the distance between opposite electrodes of the same polarity along the accelerator axis. The phases with which the distances between the electrodes vary in the xy planes are shifted by a half-period. At the same time, the periodicity of the focusing is equal to the electrode modulation period, while the acceleration period is equal to the half-period of the modulation. The squares of the distances from the electrodes to the accelerator axis vary in accordance with a sinusoidal law. An rf voltage is applied to the electrodes, and as the particles move along the axis they are successively subjected to the action of fields with alternating signs of the gradient. This leads to the appearance of a hard focusing effect in the spatially homogeneous quadrupole system. The spatial period of the variation of the distance between the electrodes must be equal to the path traversed by a particle during the rf period. The component of the electric field along the z axis is modulated, and this produces a resonant accelerating effect. Figure 4b, which shows the distribution of the longitudinal component of the electric field along the accelerator axis, reflects the circumstance that the particles trapped in the regime of acceleration at phases close to the synchronous phase φ_s are always in the accelerating polarity of the field as they move along the accelerator axis. Traveling during the half-period of the rf voltage a distance equal to the half-period of the electrode modulation, the particles arrive at the subsequent modulation half-period at the time when the field changes sign and also becomes accelerating for the particles (broken curve). In such an accelerator, the construction of the electrodes makes it possible to reduce the length of the structure period in relation to an Alvarez–Blewett accelerator and, thus, to significantly lower the injection energy. It is also important that for the same energy and apertures of the accelerators the Coulomb limit of the peak current, which is related to the transverse repulsion, is four times higher in this accelerator than in an Alvarez–Blewett accelerator, since the focusing period is halved. All this taken together makes it possible to lower the injection energy appreciably but still have a fairly high beam intensity. The rf voltage at the electrodes is excited by means of a double H resonator (Fig. 5). As can be seen from the

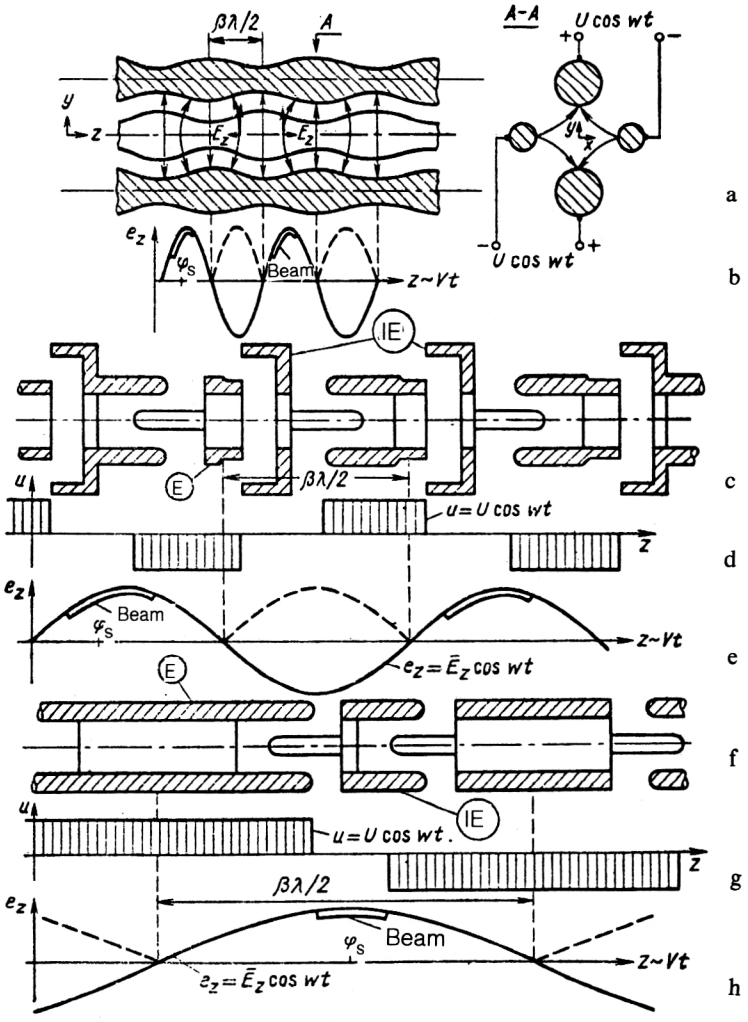

FIG. 4. Section of initial part of the accelerator: a) simplified picture of the electric field for electrode in section; b) distribution of longitudinal component of field in section of initial part of the accelerator. First section of main part of accelerator with asymmetric accelerating gap: c) shape of electrodes; d) diagram of voltage distribution on electrodes; e) first spatial harmonic of the distribution of the longitudinal component of the electric field and position of proton bunch for instant of time corresponding to equilibrium phase. Second section of the main part of the accelerator with symmetric accelerating gap: f)–h) diagrams analogous to those for the first section of the main part of the accelerator.

figure, the horizontal diametral plane divides the double H resonator into two single resonators. In turn, each resonator consists of a cylindrical tube that is cut along a generator with electrodes attached along the edges of the cut, and it is, in essence, an induction coil loaded by the capacity of the electrodes. On the line opposite the cut there is a voltage node, while at the cut there is a maximum of the electric field strength, the electric component of the rf field being mainly concentrated in the cut. The magnetic field has only a longitudinal component, except in the regions at the ends near the bottoms, where the field changes direction. The behavior of the beam in the spatially homogeneous hard-focusing channel has characteristic features. In each section along the accelerator axis, the beam has a size that pulsates in time. In each of the planes ($y=0$ or $x=0$) the maximal size of the section occurs at the time when the channel in the given plane focuses, and it has minimal size when the channel defocuses.

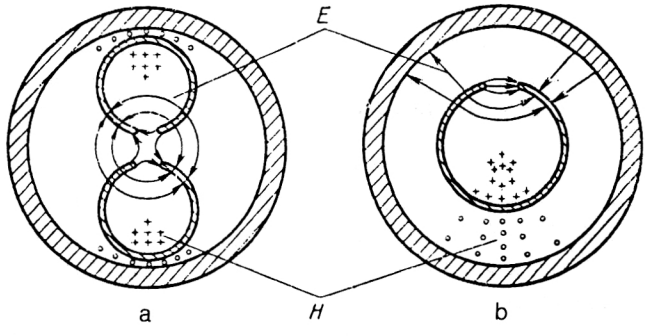

FIG. 5. Picture of rf field in H resonator: a) double H resonator of section of the initial part of the accelerator; b) H resonator of section of main part of the accelerator.

Main part of the accelerator

The accelerating system of the main part of the accelerator is divided into two sections and is made up of single H resonators loaded with drift tubes with electrodes that produce focusing of the beam by an rf field. At various times, proposals were made for constructions of accelerating systems with drift tubes in resonators with longitudinal magnetic waves permitting a reduction in the size of the accelerator, but in practical constructions difficulties arose with focusing and in obtaining a uniform field along the axis. With the appearance of the H resonator with the construction described in Ref. 8, these difficulties were to a large degree overcome.

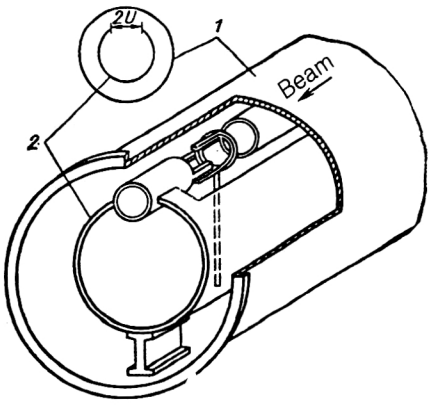

FIG. 6. Diagram of H resonator with electrodes of section of the main part of the accelerator.

Another step that made it possible to significantly improve the parameters of the structure with rf focusing by the accelerating field was the use of a double accelerating gap (Figs. 4c and 4f).[6] Between two drift tubes an intermediate electrode at zero potential was introduced. The drift tubes are fixed alternately to the left and right edge of the H resonator, and the intermediate electrodes are placed on mounts along the line with zero potential (Fig. 6). The electric fields in the accelerating gaps are, as a rule, limited by the breakdown voltage. Because of this, the single-gap accelerating interval with focusing rf field,[5] which has focusing and accelerating components, naturally has, for a given field strength, an acceleration rate that is lower than in an Alvarez accelerator. Introduction of the intermediate electrode gives a total focusing strength of two gaps that is the same as for a single gap, but because of the better configuration of the rf field it approximately doubles the efficiency of acceleration compared with the single-gap accelerating interval, and the efficiency becomes comparable to the acceleration efficiency of an Alvarez structure.[11]

In the first section of the main part of the accelerator to 16 MeV, the double-gap structure is asymmetric (Fig. 4c). With rf voltage applied to the electrodes (Fig. 4d), there is formed in the first half (in the beam direction) of the gap an axisymmetric field, i.e., the field has only an accelerating component; in the second half, there is, besides the longitudinal component, a quadrupole component formed in the space between the rods (called "horns") of the intermediate and final electrodes. At the same time, the relationship between the amplitudes and phases of the accelerating and focusing components of the field is favorable for the greater part of the bunch of particles. Figure 4e illustrates in a simplified form the acceleration of the particles in this structure. The broken curve, as in the periodic structure of the initial part of the accelerator, reflects the circumstance that the bunch of particles, coming from accelerating polarity of the field, reaches the next half-period of the electrode structure at the time at which the field changes its polarity, and thus the bunch is again accelerated. The shape of the electrodes in the axisymmetric half of the gap is chosen to make the capacitances of the two halves equal and, therefore, the field strengths on them equal. However, as the acceleration of the particles proceeds and the acceleration period grows, the horns acquire an appreciable inductance, and this makes it difficult to balance the voltages in the two halves of the gap. To reduce the influence of this, a symmetric structure of the double gap is used in the second section (Fig. 4f), in which the total length of the horns is the same but the length of an individual horn is halved, and the capacitance in the two halves of the gap is automatically the same. As regards the focusing parameters, this structure is somewhat inferior to the asymmetric form, but it is simpler to ensure balancing of the voltages on the halves of the double gap.

Some characteristics of the accelerating system

The initial and main parts of the accelerator have different accelerating structures, and the acceleration efficiency in the initial part is approximately 2–3 times lower than in the main part. The choice of the energy at the transition from the initial to the main part of the accelerator is based on a compromise between the desire to achieve overall the highest possible acceleration rate by choosing a low energy of the transition (and, therefore, shortening the total length of the accelerator) and the need to avoid resonance between the longitudinal and transverse oscillations of the beam in the main part of the accelerator at low energies. In addition, raising the energy of the transition to the main part of the accelerator makes it easier to fit electrodes with the necessary length in the acceleration period. After an analysis of all the conditions, an energy of the transition to the main part equal to 2 MeV was chosen. The choice of the energy of injection into the initial part of the accelerator was determined by the parameters of the ion gun. It is clear that if the voltage on the elements of the ion optics of the source is lower, the construction of the ion gun will be simpler. However, if the voltage is reduced below 100 kV, the conditions under which the beam is extracted from the plasma are less favorable, and the maximal current of the gun falls. Accordingly, an ion gun to 100 keV was used. The characteristics of the accelerator are largely determined by the choice of the wavelength of the rf power supply. The wavelength determines the overall arrangement and size of the accelerator, the type of oscillator tubes, the circuit of the high-power rf amplifiers, etc.

When the URAL-30 accelerator was designed, the existence of the well-developed oscillators of the rf power supply of the I-100 accelerator had a decisive influence on the choice of the wavelength $\lambda = 2$ m. A feature of the accelerating structures of the URAL-30 is that the stored energy is less than in the resonators of an Alvarez accelerator. In particular, this is also due to the fact that the H resonator has a dimension that is one third of that of an E_{010}-wave resonator when both work at the same frequency of the rf field. Because of this feature, it is necessary to introduce into the rf power-supply system of the URAL-30 devices to compensate the loss of rf energy during the working pulse of the current when intense beams are accelerated. Thus, the obvious advantage in compactness of

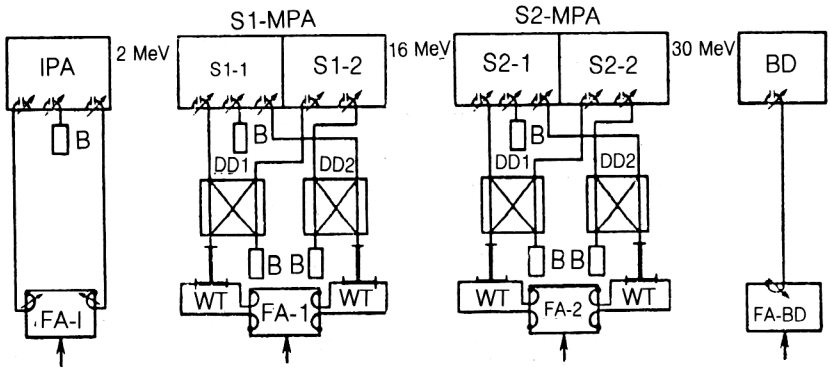

FIG. 7. The rf power supply for the accelerator URAL-30: ISA is the initial section of the accelerator; S1 and S2 are sections of the main part of the accelerator (MPA); BD is the beam debuncher; B is the ballast load; DD is a directed power distributor; WT is a matched waveguide transformer; and FA is the final rf amplifier.

the URAL-30 accelerator does result in a somewhat more complicated rf power-supply system.

A further element of the rf system of the accelerator is the beam debuncher.[12] It takes the form of a two-gap coaxial resonator and is placed at the exit from the accelerator in order to equalize the energies of the accelerated particles.

The rf power-supply system

To introduce rf power into the initial part of the accelerator and the sections of the main part, a scheme was chosen with excitation of the resonators distributed over the length of the accelerator and branching of the rf circuit at a high power level (Fig. 7). The excitation circuit consists of a master oscillator, preamplifiers, and high-power final amplifiers. The phase regulation between the initial part of the accelerator, the sections of the main part, and the debuncher is done by means of phase shifters. In the initial part, there are two power-supply points, four in each of the sections of the main part, and one in the debuncher. From a final amplifier FA, in which GI-27 AM triodes are used, the power is directed from two outputs of the amplifier to feed the resonators. The power is supplied through coupling loops that can be smoothly regulated and have automatic compensation of the self-inductance in any position of the loop. The compensation occurs through the introduction of a series capacitance; as the changes of the loop area are regulated, this is changed in accordance with a specially chosen law, which ensures that the series circuit is tuned to resonance.

Power is introduced into the initial part of the accelerator from a final amplifier through two symmetric coupling channels, which include cable lines and regulated elements of coupling from the final amplifier to the initial part of the accelerator. Power is introduced into the debuncher from an individual final amplifier through one coupling channel.

The sections S1 and S2 of the main part of the accelerator have identical power supplies, constructed symmetrically. The power is taken from two final amplifiers by four symmetric coupling loops connected to matching waveguide transformers WT. The power is passed from the WT outputs to the inputs of directed distributors DD, at the outputs of which the power is halved. The power passes from the DD outputs to the sections of the main part of the accelerator through cable lines with coupling of equal phase length. The rf fields in the subsections of each of the sections S1 and S2 are shifted in phase by $\pi/2$ with phase lag along the path of the beam. The shunt resistors of the subsections are equalized by loading the subsections with ballast loads *B*. In this supply scheme, the regime of the final amplifiers does not depend on the loading of the rf field of the section by the beam.[13] Indeed, for a certain beam current one can obtain a regime of matched loading by the resonator. Changes in the current lead to a perturbation of the input impedance of the subsections and reflection of the wave from the resonator entrance; the reflected wave passes through the uncoupled arms of the DD to the ballast load, and this ensures constancy of the regime of the final amplifiers independently of the changes in the loading of the resonator by the beam.

The particle dynamics limits the tolerances for the instability of the accelerating fields in the initial and main parts of the accelerator as follows: in amplitude not more than $\pm 2\%$, and in phase not more than $\pm 3°$. The energy stored in the *H* resonators is low, and therefore the acceleration of intense beams (~ 100 mA) of long duration (more than 1 μsec) requires compensation of the loss of rf energy. To this end, rapid compensation of perturbations

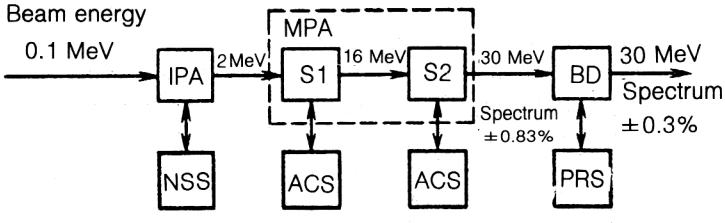

FIG. 8. Block diagram of the accelerator URAL-30 with systems for compensating perturbations of the rf field: IPA is the initial part of the accelerator; S1 and S2 are the sections of the main part of the accelerator (MPA); BD is the beam debuncher; NSS is the nonlinear stabilization system for the rf field; ACS is the autocompensation system for the perturbations of the rf field; PRS is the parameter and regime selection system.

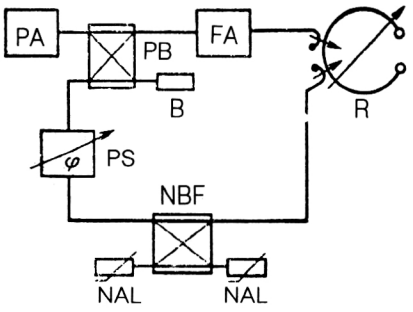

FIG. 9. Block diagram of nonlinear stabilization system: PA is a preamplifier; PB is the power-addition bridge; R is the resonator; B is the ballast load; PS is the phase shifter; NBF is the nonlinear bridge four-terminal network; NAL is the nonlinear adjustable load.

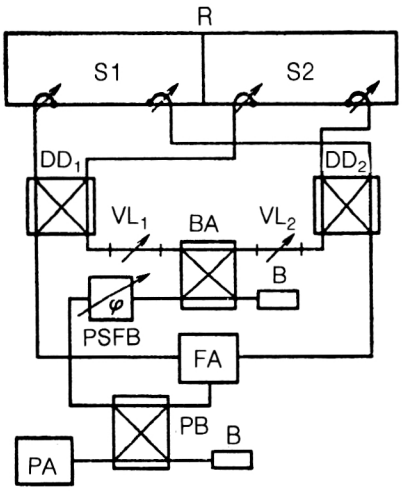

FIG. 10. Block diagram of autocompensation system for perturbations of the rf field: R is a resonator of the main part of the accelerator; S1 and S2 are the subsections of the resonator; DD is a directed power divider; VL is a variable-length line; BA is a bridge signal attenuator; PSFB is the phase shifter of the feedback circuit; B is the ballast load; PB is the power-addition bridge; PA is a preamplifier; FA is a final amplifier.

of the rf field by the beam is achieved as follows (Fig. 8). In the initial part of the accelerator, a nonlinear stabilization system carries out autoregulation on the basis of the signal of the rf voltage in the resonator (Ref. 14); in each section of the main part of the accelerator, there is an autocompensation system ACS with autoregulation in accordance with the signal of the wave reflected from the resonator (Ref. 15); in the debuncher, there is a method for selecting the parameters and regime PRS in the rf power-supply circuit. In the nonlinear stabilization system NSS (Fig. 9), a high dynamical coefficient of stabilization of the rf field amplitude is achieved by including in the feedback circuit, which includes a final amplifier, a nonlinear four-terminal network, the distinctive property of which is a dependence of the transfer coefficient on the voltage at the input, which, in its turn, is proportional to the level of the rf field in the resonator. The current–voltage characteristic of the four-terminal network must, ideally, have a relay form. The nonlinear four-terminal network is based on a double T bridge NBF, to the input of which the feedback signal from the resonator is sent. Two uncoupled arms of the NBF are loaded with nonlinear adjustable loads NAL, in which GI-39B triodes are used. The working point in the current–voltage characteristic of the NAL is chosen in such a way that for the nominal level of the field in the resonator the input resistors of the loads are matched to the arms of the T bridge and there is no signal at the feedback output; all the power reaching the input of the NBF from the resonator is dissipated in the NAL. If the amplitude of the rf field deviates from the nominal value, the working point is displaced on the current–voltage characteristic of the triode, and the internal resistance of the triode is changed. The loads are no longer matched, and an appreciable fraction of the power passes from the NBF output to the feedback circuit. The feedback circuit contains a phase shifter PS for initial phasing of the feedback ring and a waveguide power-addition bridge PB to add the signals of the preamplifier and the feedback circuit. The gain of the final amplifier is controlled by the difference signal. The maximal coefficient of stabilization of the rf field amplitude is determined by the stability of the system, and for the chosen parameters of the nonlinear stabilization system is 20–25. The coefficient of stabilization of the phase by means of the nonlinear stabilization system is characterized by the static parameters of the system and does not exceed 2.

A block diagram of the autocompensation system in the sections of the main part of the accelerator is shown in Fig. 10. The reflected wave separated by means of the directed distributor DD is added in the waveguide addition bridge PB to the reference signal from the preamplifier with definite phase relations that are regulated by the phase shifter of the feedback circuit (PSFB). The resultant wave will be the regulating signal for the final amplifier FA, and the autocompensation system will reduce the amplitude and phase of the rf field to steady values. The initial tuning requires addition of waves in the addition bridge PB with definite amplitudes and phases regulated independently of each other. The principle of phase-independent regulation of the rf field amplitude is solved in this scheme as follows. The reflected waves, of equal amplitude, from the uncoupled arms of the directed power distributors DD_1 and DD_2 reach the inputs of the bridge attenuator BA through the variable-length lines VL_1 and VL_2. A property of the bridge scheme of power addition is the possibility of complete redistribution of the power from one output arm to the other, depending on the phase difference at the output of the bridge attenuator. By increasing the phase length of VL_1 and decreasing by the same amount the phase length of VL_2, the required redistribution of power between the feedback line and the ballast load B can be achieved. At the same time, the phases of the signals at the outputs of the bridge attenuator remain constant.

For open feedback of the autocompensation system, the perturbations of the rf field in the main part of the accelerator when the beam current is 80–100 mA reach 14–16% at 1–2 μsec after entrance of the beam, and this leads to a sharp decrease of the accelerated current. When

TABLE I. Basic parameters of the linear accelerator URAL-30.

Parameter	Value		
		MPA	
	IPA	1st section	2nd section
Injection energy, MeV	0.1	2	16
Output energy, MeV	2	16	30
Beam current, mA	-	-	Up to 100
Momentum spread of particles in beam $\pm\Delta p/p$, %;			
without debuncher	3.2	1.2	0.83
with debunhcer	-	-	0.3
Normalized emittance (90% of current), mrad·cm	-	-	0.6π
Duration of current pulse, μsec	-	-	Up to 10
Number of pulses in packet	-	-	32
Repetition frequency of pulses in packet, Hz	-	-	20
Repetition frequency of packets, Hz	-	-	0.2
Working frequency of rf field, MHz	-	-	148.5
Steady power of generators, MW	1.1	3.1	4.1
Relative velocity of synchronous particle, V_s/c	0.0146–0.0648	0.0648–0.1830	0.1830–0.2465
Structure of focusing period	FD	FDDF	FDDF
Diameter of aperture $2R_a$, mm	20.22–16.00	19.00	22.00
Length of resonator, m	3.383	8.359	12.142
Internal diameter of resonator $2R$, mm	180	222	242
Length of acceleration period ($\beta\lambda/2$), mm	14.2–64.7	65.6–183.5	184.8–247.5

the autocompensation system is switched on, acceleration of a beam with current up to 100 mA and with residual perturbation of the field in amplitude of 4–6% and in phase of 3–4° is ensured. The rapid-stabilization system in the debuncher is based on the parameter and regime selection method (PRS) in the rf power-supply scheme. A certain initial regime of the final amplifier is established, and then, if there is underloading of the rf field by the beam, the amplifier is automatically programmed to correct the phase and amplitude of the field in the resonator under the assumption that the effect of the beam on the field has a regular nature. Use of the PRS method made it possible, for beam current 100 mA, to reduce the phase instability of the rf field from 3.8 to 1.4° and the amplitude instability from 7 to 3.2%, and to obtain an energy spectrum of the beam at the output within the limits ±3%. Slow perturbations of the rf field in the accelerator are compensated by stabilizing the supply voltages, thermostatic control of the resonators, and autotuning of the phase in the channels of the rf system.[16]

Basic characteristics of the linear accelerator URAL-30

The accelerator URAL-30 was first commissioned in 1977. Since then, individual systems have undergone some modernizations and improvements. In 1981, the beam from the linear accelerator was injected into a booster. Circulation of protons with energy 30 MeV in the IHEP booster was obtained. Since 1983, the URAL-30 accelerator has operated as an injector to the booster. The main parameters of the accelerator are given in Table I.

2. THE BOOSTER

The booster is the first in the series of IHEP synchrotrons: cyclic accelerators.

The need to build the booster in order to raise the beam intensity in the U-70 accelerator arose from the development of a program of neutrino research at the IHEP. If one is studying the interactions of particles with small cross sections, the beam intensity may determine the very possibility of making an experiment during a reasonable time scale. Restrictions on the intensity of the accelerated beam in the U-70 are imposed by the permissible shift of the betatron frequencies under the influence of the beam self-field at the initial energy of the particles in the accelerator, i.e., the injection energy. For the existing parameters of the U-70, an injection energy of more than 1 GeV corresponds to the required intensity 5×10^{13} protons/cycle of the accelerated beam. Different possibilities of high-energy injection into the U-70 accelerator were analyzed,[17] and preference was given to a rapid booster to 1.5 GeV, i.e., to a small-radius synchrotron operating with high repetition rate and filling the main accelerator with protons during a few of its cycles. In view of the allowed Coulomb shift of the betatron frequencies in the booster, the energy of injection into the booster should not exceed 30 MeV. A significant increase of it is not expedient, since the growth of the particle velocity means that a greater number of revolutions is required on injection in order to accumulate the same charge.

For convenience of synchronizing the booster to the main accelerator U-70, it was necessary to choose an approximately multiple ratio of their lengths. The wish to make the perimeter of the booster as short as possible is restricted by the requirements on the parameters of the

magnetic field and difficulties associated with the accumulation of a large number of particles on a short path. For this reason, the length of the booster perimeter was taken to be 99.16 m, which is 1/15 of the length of the main U-70 accelerator. For the chosen multiplicities of the radio frequencies of the booster and the U-70, 1 and 30, respectively, each bunch accelerated into the booster is injected into one separatrix of the main accelerator, for the filling of which 30 injection cycles are thus required. For this method of injection, 1.7×10^{12} particles must be accelerated in each booster cycle. The maximal repetition rate of the booster is chosen to be 20 Hz; an increase is hindered by difficulties associated mainly with greater complexity of the accelerating system. Thus, the parameters of the accelerator were chosen in such a way that the critical energy of the booster (the energy at which the longitudinal oscillations of the particles in the beam lose stability) was above the nominal value. Calculated characteristics of the longitudinal and transverse motions of the particles in the booster, and also the requirements on the parameters of the accelerating voltage and the magnetic field are given in Refs. 18 and 19. The physical commissioning of the booster occurred in 1983, during which individual and global adjustments of the booster systems were made; on October 28, 1983 accelerated protons with energy 1.5 GeV were obtained.

Magnetic system of the booster

The circular electromagnetic system of the booster[20] has separate beam circulation and focusing functions and is a magnetic system with strong focusing. The circular electromagnet consists of 12 triplets of quadrupole lenses and 24 dipole bending magnets, which together form 12 periods of the magnetic structure. Five of the bending magnets have an extended horizontal opening and are situated in regions of beam injection and extraction. Each dipole magnet consists of two packets glued from electrotechnical steel and united by a single coil. The nonlinearities in the fields of the magnets are corrected by end elements. The rms deviations of the field in the magnets and of the gradient in the lenses do not exceed 0.2%. The free spaces between the main elements of the circular electromagnetic system of the booster are occupied by resonators of the accelerating system, the magnetic systems of the beam injection and extraction, correcting magnetic elements, and other equipment.

The booster is equipped with a well-developed system for correcting the magnetic field, by means of which the following characteristics can be regulated during the accelerating cycle: the shape of the equilibrium orbit in the horizontal and the vertical, the frequency of the betatron oscillations, the dependence of the betatron frequencies on the oscillation amplitude of the particles, and the band widths of certain betatron resonances.

The correction system[21] contains 22 special correcting magnets, and also additional coils of the focusing and defocusing blocks of the main magnet, by means of which the frequencies of the betatron oscillations are regulated. The magnetic circuit of the correcting magnet is made of mixed

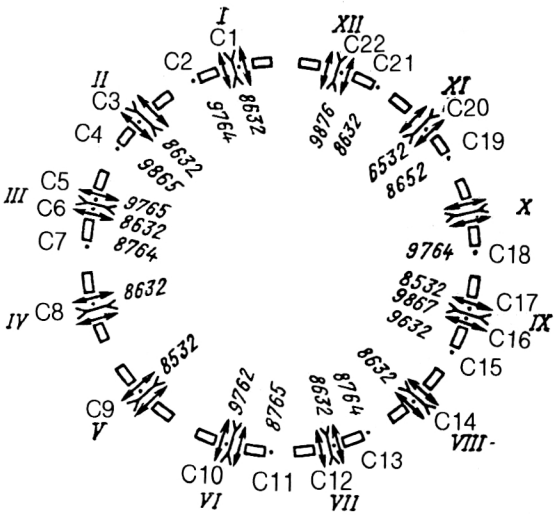

FIG. 11. Arrangement of elements of magnetic system of the booster: ▭ is a dipole magnet; ↕ is a focusing quadrupole magnet; ⟩⟨ is a defocusing quadrupole magnet. The numbers identify the types of correction coils C1–C22: 2 for dipole, 4 for quadrupole, 6 for sextupole, 8 for octupole; 3, 5, 7, 9 are for the corresponding skew dipole, quadrupole, etc.

transformer steel and has a cylindrical inner surface, along which four sets of coils of different multipolarities are arranged layer after layer. Altogether, there are 12 types of corrector. The arrangement of the main magnetic elements of the ring and correctors is shown in Fig. 11.

We give the main parameters of the magnetic elements of the booster:

Number of dipole magnets	24
Induction of the magnetic field, T	0.139–1.31
Number of magnetic lenses:	
focusing (F)	24
defocusing (D)	12
Type of magnetic structure	MOFODOFOMO
Number of periods of magnetic structure	XII
Gradient of magnetic field in lenses, T/m	1.13–10.67
Effective lengths, m	
magnet	1.5
focusing lens	0.33
defocusing lens	0.5714
Number of correcting magnets	22
Total number of correcting coils (normal and "oblique"):	
dipole	24
quadrupole	11
sextupole	29
octupole	24
Amplitude of fundamental harmonic of the field in the corrector (for current 150 A in coil)	
in dipole, T	0.026

in quadrupole, T/m	0.3
in sextupole, T/m^2	2
in octupole, T/m^3	23
Effective aximuthal length of corrector, mm:	
dipole	300
quadrupole	275
sextupole	275
octupole	300
Opening of chamber in blocks ($r \times z$), mm	140×61

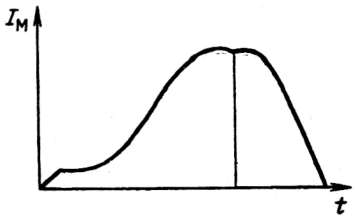

FIG. 12. Diagram of current in coil of ring magnet of the booster.

Power-supply systems of the ring electromagnet and correcting magnets

There are specific requirements for the power-supply system of the ring electromagnet.[22] The booster operates in a boxcar stacking regime, successively filling 30 separatrices of the main accelerator U-70. At the same time, the injection process occupies an appreciable fraction of the operating cycle of the main accelerator. It is obvious that the accelerator efficiency will be improved if the cycling frequency of the booster operation is raised. However, a simple increase of the frequency and, therefore, rate of growth of the magnetic field is limited by the capabilities of the high-frequency accelerating stations. Therefore, the power-supply system of the booster electromagnet is based on a schematic solution that ensures a relatively slow growth of the magnetic field in the working part of the cycle and then a rapid decrease of the magnetic field to zero. The supply system generates single-polarity current pulses (Fig. 12) by controlled discharge of condenser batteries to the inductance of the magnet coils. A decrease of the current pulse duration in the ring electromagnet is achieved by shortening the leading edge of the pulse through a step change of the parameters of an LC circuit. This is done by means of a circuit that commutates the electromagnet coils to series connection at the leading edge of the pulse and to parallel connection at the trailing edge. The coils of all blocks of the electromagnet are divided into four groups EM_1–EM_4 (Fig. 13). Within a group, the coils are connected in series. Two groups form a commuting pair: EM_1, EM_2, (EM_3, EM_4,). At the leading edge of the pulse, the coils of this pair are connected in series; at the trailing edge, in parallel. Each pair is connected to the other in series and forms with the reservoir capacitors C_0 a series ring LC circuit. The electrical supply and commutation circuits of each pair of coils are identical. The basic arrangement of one half of the ring circuit of the power-supply system of the booster electromagnet[23] is shown in Fig. 13. When the synchronization pulse for starting the accelerator cycle arrives, the thyristor switches T_1, T_7, and T_9 are activated. The reservoir capacitor C_0 is discharged to the injection choke coil Ch_1 and the coils of the blocks, which are connected in series. When the injection current is reached, the thyristor switch T_5 is activated, and the precharged capacitor C_1, on which the voltage has polarity opposite to that on C_0, is connected to the electromagnet coil. The initial voltage on the capacitor C_1 is established during the previous pulse at a level to ensure a derivative of the current on the injection area close to zero. The capacitor C_0 continues to be discharged through the choke coil Ch_1, giving energy to the capacitor C_1 and the electromagnet. At a definite time, the switch T_3 is activated, and the capacitor C_0 is recharged through the choke coil Ch_2 to a voltage of opposite polarity, the value of which is chosen to ensure during the next stage of the cycle reliable blocking of the switches T_7 and T_9 and breaking of the series connection of the electromagnet coils. After the recharging current pulse through Ch_2 and the charging current pulse through Ch_1 have ended, the thyristor switches T_1, T_3, and T_5 are closed, and the current of the electromagnet flows only through the capacitor C_1.

When the voltage on the capacitor C_1 falls to the level necessary for injection in the following cycle, the diode-thyristor switches DT_1, DT_3, DT_5, DT_6, DT_7 are activated, resulting in commutation of the coils EM_1, EM_2 to parallel connection, formation of the current pulse decay, and res-

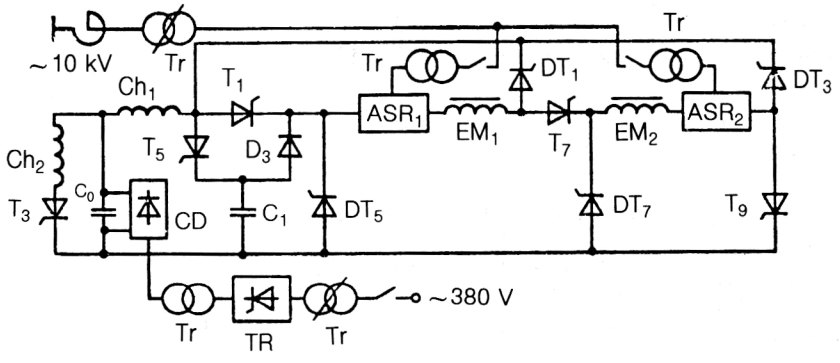

FIG. 13. Block diagram of main power-supply system of ring electromagnet of the booster: EM_1–EM_4 are groups of coils of the ring electromagnet; Ch are chokes; Tr are transformers; T are blocks of thyristor switches; DT are blocks of diode–thyristor switches; ASR are additional supply rectifiers; TR is a thyristor regulator; CD is a charging device.

toration of the energy to the capacitor C_0 during a time that is approximately half the current rise time.

The stability of the current in the electromagnet is maintained by two stabilization systems[24]—fast and slow. The fast stabilization circuit contains four thyristor rectifiers for additional power supply, ASR_1–ASR_4 (matching the number of groups of electromagnet coils), each of which is designed for nominal voltage 700 V and current pulse amplitude 4000 A. The voltage levels of all of the rectifiers is corrected simultaneously on the basis of results of measurement of the current amplitude of the preceding pulse in the packet.

The slow stabilization circuit consists of the thyristor regulators TR, which are on the primary side of the rising transformers Tr, which power the charging devices CD of the capacitor batteries C_0. This system corrects the discharge voltage level of the capacitor C_0 once during the formation of the packet of pulses using the results of measurement of the amplitude of the first pulse in the packet.

The power-supply system of the magnetic correctors consists of individual sources, each of which powers an individual corrector coil. The reference voltage for the power source is supplied by a digital-to-analog converter, for which the digital code is formed by a function generator. The function generator is controlled by an EC-1010 computer through a SUMMA frame. In all the power-supply sources there is an automated control of the current within given tolerances in each acceleration cycle.

The basic parameters of the power-supply source of the ring electromagnet of the booster are as follows:

Maximal current, A	4000
Injection current, A	415
Number of pulses in packet	Up to 32
Pulse duration relative to base (at cycle repetition rate of about 16.6 Hz), msec	About 57
Required stability of current from pulse to pulse	2×10^{-4}

Accelerating system of booster

The rf acceleration system of the booster consists of a programmed master rf oscillator with apparatus for frequency autocorrection based on the beam position in the vacuum chamber[25] and nine accelerating stations (Ref. 26): power amplifiers. Each of these is loaded to an accelerating device, which takes the form of two resonators excited in antiphase with a common gap and tuned in frequency by the magnetization of ferrite cores in the resonator. The master oscillator forms rf voltages programmed in frequency and amplitude, the phases being shifted by angles that are multiples of 30° in accordance with the arrangement of the resonators around the accelerator perimeter. Signals from a functional converter, a beam feedback system, and a system for synchronizing the beam extraction are sent to the master oscillator, which is controlled by a voltage. This ensures the necessary functional dependence of the frequency of the accelerating rf voltage on the magnetic field induction, on the position of the beam bunches with respect to the radius, and relative to the equilibrium phase of the rf field. The nonlinear dependence of the frequency of the accelerating voltage on the magnetic field is formed by means of the functional converter, to the input of which a signal from a magnetic field sensor fixed in a gap of the ring electromagnet is sent. The position of the beam is monitored by electrostatic electrodes placed in the vacuum chamber of the accelerator. The accelerating system operates in a boxcar stacking regime. The nominal acceleration regime is ensured by the operation of six stations. If their number is greater, the level of the rf voltage in the resonators is reduced accordingly. The dynamics of the rearrangement of the resonator at the start of the acceleration cycle is strongly influenced by the transient process in the ferrite core produced by the decays of the magnetization current after the end of the preceding cycle; this transient process leads to a lowering of the initial frequency of the resonator by about 100 kHz. To reduce this effect, several conditioning cycles of the magnetization current are applied to the resonators before the start of the packet of working cycles in order to control the transient process in the core; there is also an anticipatory programmed increase of the current at the beginning of a cycle. Besides the traditional systems for amplitude autoregulation and frequency autotuning of the resonator, a wide-band negative feedback with respect to the radio frequency is used in the final cascade of the station. It ensures a widening of the transmission band of the rf system, which is needed for the operation of the beam feedback system and increases the stability of the regulation systems in the case of an intense beam.[27]

The basic parameters of the booster accelerating system are as follows:

Steady rf power of an accelerating station, kW	60
Revolution frequency, MHz	0.7467–2.791
Maximal voltage in resonator gap, kV	About 10
Number of accelerating stations	9

Vacuum system

As the beam is accelerated, the particles are scattered by molecules of the air gases, which degrades the beam parameters. This effect can be reduced to a minimum by evacuating the ring chamber of the accelerator. For the booster, the required level of the vacuum is about 5.3×10^{-5} Pa ($\sim 4 \times 10^{-7}$ mm Hg). For the injection and extraction beam lines these requirements are less stringent because the particle path length in the transporting channels of the booster complex are much shorter than the path traversed by the particles as they are accelerated in the ring

chamber of the booster, and, therfore, there is less matter on the beam path.

The vacuum system[28] of the booster complex consists of the vacuum ring chamber of the accelerator, the ion guide of the injection channel connecting the booster to the linear accelerator, and the ion guide of the channel through which the beam is extracted from the booster. The evacuated ring of the booster includes several types of vacuum chamber, the constructions of which naturally correspond to the position of the elements of the periodic magnetic ring system and the position of the accelerating stations, bump magnets, etc., around the ring perimeter. The main elements in this system are the vacuum chambers of the bending magnets and the quadrupole lenses (with internal measurements 61×150, 61×190, and 88×184 mm), which largely determine the requirements on the parameters of the vacuum ring system. The chambers are corrugated and made of stainless steel of the mark 12Kh18N10T with thickness 0.25 mm. The vacuum chamber of an accelerating station is made of a tube of oval section, which is simultaneously the resonator wall. The material of the tube is electrotechnical steel, and the accelerating gap is insulated by a ceramic insertion. Special vacuum boxes are used to hold the bump magnets, and also other equipment. The elements of the vacuum system are mainly joined by means of quick-disconnect vacuum junctions with metallic seals. Special requirements on the construction of the vacuum junctions are imposed by operations under conditions of appreciable eddy currents in the walls of the vacuum chambers that arise because of the rapid rates of change of the magnetic field during the acceleration cycle. The severe distortions that these currents can introduce in the guiding magnetic field make it necessary to undertake special measures to limit them. For this, the vacuum chambers of the bending magnets are electrically decoupled from the remaining vacuum chambers by covering the connecting collars with insulating enamel, and the poles of the magnets are insulated from the vacuum chamber by means of glass-reenforced plastic linings.

The ion guides of the injection and extraction channels are made of tubes of internal diameter 134 mm made of stainless steel of the mark 12Kh18N10T. There are special vacuum chambers in the deflecting magnets of the injection and extraction sections. In the majority of cases, the elements of the vacuum system of the beam transport channels are also joined by means of special quick disconnect junctions. For convenience of assembly and use, the individual vacuum elements of the transport tracts are joined by means of flexible sylphon bellows.

The vacuum regions of the booster are evacuated to pressures $\sim 10^{-3}$ Pa by preliminary vacuum stations, each of which consists of a mechanical forevacuum NVZ-20 pump and a TMN-200 turbomolecular pump. The high-vacuum evacuation is done by means of magnetic-discharge pumps of the types NMD-0.25 and NMD-0.4. The average working level of the vacuum in the ring chamber of the booster is 2.7×10^{-5} Pa. The enhanced release of gas in the region of the septum magnets and bump magnets leads to a nonuniform distribution of the vacuum level

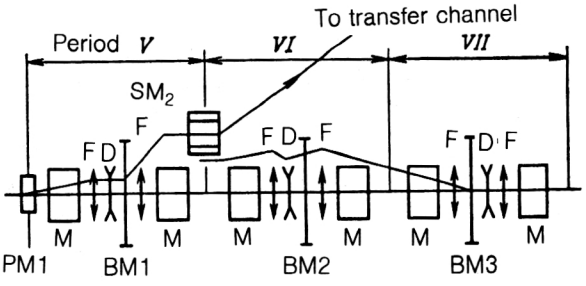

FIG. 14. Arrangement of equipment of booster injection system: SM is a septum magnet; PBM1–PBM4 are pulsed bump magnets; M are dipole magnets of the ring electromagnet; F and D are, respectively, focusing and defocusing quadrupole lenses of the booster ring.

round the ring of the accelerator; it fluctuates in the range $(1–9)\times10^{-5}$ Pa.

One of the important functions of the vacuum system of the booster is reliable control of the vacuum level. This is indicated by vacuum meters of the type VMB-8, and when the pressure in the ring chamber rises above the level 1.3×10^{-3} Pa (10^{-5} mm Hg) there is an automatic switching off of the accelerating stations and the bump magnets. If there is a further worsening of the vacuum above pressures 5×10^{-2} Pa, the power supply of the magnetic-discharge pumps is switched off, and sliding shutters close off the section in which the fault has occurred from the remaining vacuum space.

System for injecting the beam into the booster

Two injection regimes are foreseen in the booster: a single-turn regime and a multiturn regime (with the number of injection revolutions up to eight). The injection system includes a magneto-optical channel that forms a beam with given parameters, bump magnets, which produce a local distortion of the booster orbit (bump) at the beam injection position, and a magnet with current baffle (septum magnet), which deflects the beam into the orbit. The arrangement of the equipment of the injection system is shown in Fig. 14.

As an example, we consider the process of two-turn[29] injection of the beam into the booster. The injection process is illustrated by Fig. 15, which shows the position of the beam on the phase plane in a section of the septum-

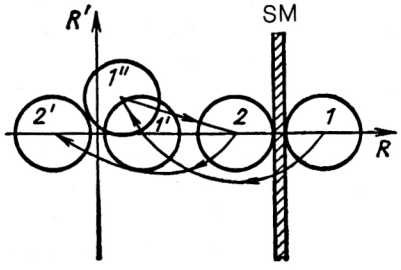

FIG. 15. Arrangement of filling of the phase space in the case of two-revolution injection (SM is the septum-magnet barrier).

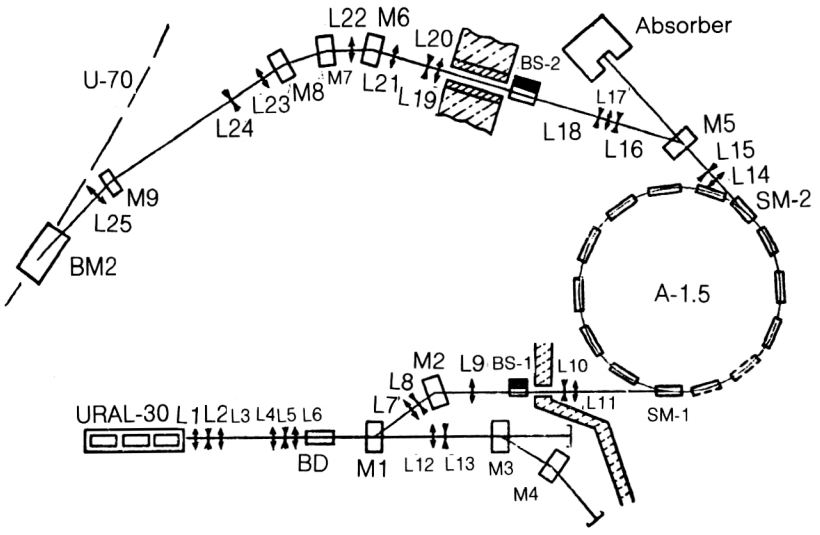

FIG. 16. Arrangement of equipment of the systems for beam injection into the booster and extraction of beam to the U-70 accelerator: M are magnets; L are quadrupole lenses; BM is a bump magnet; SM is a septum magnet; BS is a beam shutter; and BD is a beam debuncher.

magnet azimuth. The beam, in position 1, is transferred by means of the two bump magnets PBM1 and PBM2, which are pulsed from a single source, to the position 1′. At the end of the first revolution the beam has been moved by the betatron motion to the position 1″, and by means of the second pair of bump magnets PBM3 and PBM4 is transferred to position 2, which is right next to the support of the septum magnet. In the second revolution, beam 2 and beam 1, which continues to arrive from the septum magnet, are acted upon by the first pair of bump magnets PBM1 and PBM2, and are shifted to the positions 2′ and 1′, respectively, after which the injection stops. The two beams are injected symmetrically with respect to the equilibrium orbit.

The magneto-optical channel[30] (Fig. 16), through which the beam is transported from the linear accelerator, includes the following apparatus. At the channel entrance, there is a doublet of quadrupole lenses (not shown in the figure), the symmetry planes of which are turned through 45° relative to the horizontal plane. These lenses are needed because, for constructional reasons, the focusing in the linear accelerator is done in planes at 45° to the horizontal. The focusing by these lenses ensures that at the entrance to the main part of the channel there is an axisymmetric beam in which there are no distinguished planes. The two following triplets of quadrupole lenses, L1–L3 and L4–L6, are used to match the emittance of the injected beam to the acceptance of the booster. The beam is transported to the entrance septum magnet of the booster by means of an achromatic optical scheme, which includes two bending magnets M1 and M2 and quadrupole lenses L7–L11. The lens regime of this part of the channel is not changed when optimal injection parameters are chosen. The section containing the lenses L12 and L13 and the magnets M3 and M4 is used to measure the beam characteristics. The beam spectrum is measured when the magnets M3 and M4 are switched on; the emittance is measured on the straight branch (magnet M3 switched off). A pulsed power supply of the magnet M1 is foreseen; this makes it possible to omit in the measuring section of the channel the required number of beam current pulses from the series of pulses developed by the linear accelerator. The quadrupole lenses are powered by stabilized current sources that ensure stability at the level $\pm 0.1\%$ in the range of working currents (20–100 A) of the lenses. The bending magnets are powered by standard IST 500 A/230 V current sources with stability 10^{-4}. All the power sources of the channel and the currents are controlled by means of an EC-1010 computer.

The beam is injected into the ring vacuum chamber by means of a septum magnet that has aperture 60×80 mm and length 0.5 m. At working current 10.5 kA, the deflection angle of the beam in the septum magnet is 8.5°. The bump magnets[31] of the booster have constructions of the same type. The magnet aperture, with rectangular cross section 130×140 mm, is formed by the poles of a magnetic circuit of ferrite cores of a C shape. The excitation winding is a busbar system consisting of an inner busbar at a high potential and an outer grounded busbar. The required current pulse is formed in the coil under the condition of matching of the wave resistances of the receiving, transmitting, and shaping lines, the lines being represented in the form of devices with distributed parameters. To achieve this, condensers are connected to the magnet excitation winding uniformly along its length. This results in the formation of a long line with the required characteristic resistance (8 Ω for PBM1–PBM3 and 16 Ω for PBM4).

The bump magnets are powered from pulse-forming lines with storage condensers, which are discharged to the magnets through high-power thyratron switches. The charging voltage is stabilized in the lines by transformer thyristor regulators at a level 15–50 kV with error 10^{-3}.

The efficiency of single- and two-turn injection of the beam into the booster is very close to 100%. For emittance of the injected beam of 4π cm·mrad, the effective emittance of the accumulated beam is 22π cm·mrad, approximately half the radial acceptance of the vacuum chamber of the booster.

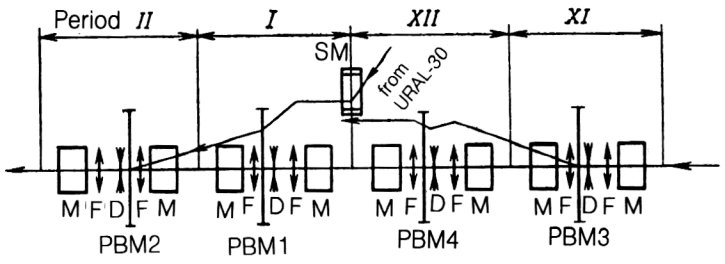

FIG. 17. Arrangement of equipment for system of beam extraction from the booster: SM is a septum magnet; PM is a pulsed magnet; BM is a bump magnet; M are dipole magnets of the ring electromagnet; F and D are, respectively, focusing and defocusing quadrupole lenses.

Systems of beam extraction from the booster and injection into the U-70 accelerator

The booster is equipped with a single-turn system for extracting the accelerated beam.[20] It consists of three bump magnets and a bump magnet which shifts the beam to the extraction septum magnet, which, in its turn, deflects the extracted beam into the transfer channel. The beam is transported through the magneto-optical transfer channel to the main accelerator U-70, where it is injected into the vacuum chamber of the accelerator by means of a multisection bump magnet. Bump magnets (BM1–BM3) are situated in 5–7 magnetic periods of the booster (Fig. 17) and produce at the end of the acceleration cycle a local perturbation of the orbit, the greatest value of which is in the region of the extraction septum magnet. The bump magnets for extraction of the beam from the booster (PM1) and its injection into the U-70 accelerator (PM2) have a construction similar to the bump magnets of the injection system, but consist of five and 18 sections, respectively, these being situated in large gaps of the accelerator. The sections are powered in the same way as in the injection system, by discharge of pulse-forming lines through thyratron switches. As a long shaping LC line, cable segments connected in parallel are used. There are relatively more stringent requirements on the rise time of the bump magnet PM2, the duration of which must not exceed 80 nsec to avoid perturbation of the motion of bunches injected earlier into the U-70 accelerator. To achieve a steeper front, peaking lines with saturated magnetodielectric (ferrite rings) are used. The peaking lines are constructed in the form of segments of coaxial lines. The PM1 and PM2 pulse-forming lines are charged by devices with transformer-transistor regulator, which ensure linear charging of an accumulator in accordance with a given digital program code, stabilization at the level 10^{-3}, and complete disconnection from the line when it is discharged.

The channel for transferring the beam to the main accelerator (Fig. 16) contains 11 quadrupole lenses and four bending magnets. The lenses L14 and L15 and the magnet M5 are used to compensate the beam dispersion at the booster exit. Two triplets, L16–L21, ensure that the emittance of the extracted beam matches the acceptance of the U-70 accelerator. The regime of the final part of the channel (the magnets M6–M8 and lenses L22–L24) is arranged to ensure matching of the dispersions of the channel and the main accelerator. At the entrance to the main accelerator, the beam transverses an appreciable distance in stray magnetic fields. To compensate their effect, the fifth gap of the U-70 accelerator contains a small pulsed magnet M9 and lens L25, and in the sixth gap of the accelerator there is a bump magnet PM2, which injects the booster beam into the vacuum chamber. Five double magnetic correctors are used for fine adjustment of the beam in the channel. In the case of autonomous adjustment of the booster, the magnet M5 is not switched on, and the beam is transported to an absorber, which is a steel cube of side 2.6 m.

Systems of automated booster control

Automation of the control systems in the booster is achieved by means of two EC-1010 minicomputers and MÉ-80 microcomputers distributed through the apparatus. One EC-1010 computer is used solely to develop the program for controlling the microcomputers. The minicomputers must perform the main computational tasks and maintain the programs of the measured data, and also serve the interface with the operator at the accelerator panel. The microcomputers implement data collection that is synchronized with the acceleration process and control system parameters that do not require appreciable calculations; they also ensure adjustment of systems from local terminals. In addition, the MÉ-80 are used to serve the operator panels and the instruments for graphical presentation of information. The computational complex is organized[32] in such a way that it ensures connection of each minicomputer to four branches through seven frames of the VEKTOR-SUMMA apparatus; a microcomputer can be placed in any of the frames. Information is exchanged between the frames and base minicomputers through parallel lines at a rate 300 kbyte/sec over distances up to 80 m.

For some parameters it is necessary to control the dynamics of the variation of the values during the acceleration cycle. This means that there is no possibility (from the sum of all such information) to use for this purpose the minicomputers or microcomputers, both on account of the limitations on the rate of data transmission and the size of the operative memory of the computers. Therefore, wide use is made in the automated system of measurement and control models with built-in buffer memory, the information transfer with these being done in a regime of block transfer with uniform loading of the main lines in time. Information about the instantaneous state of the booster systems is entered automatically, without operator demand, into the working data base after each cycle packet. The necessary data from the working base are used by the application programs without recourse to the apparatus or

is stored on magnetic tape for subsequent analysis of the booster operation regimes.

Basic parameters of the ring injector booster at the IHEP

Energy of protons, MeV	30–1500
Pulse intensity (projected), proton/cycle	1.7×10^{12}
Intensity achieved by December 1988, proton/cycle	0.9×10^{12}
Number of cycles in packet	Up to 29
Cycle repetition frequency, Hz	Up to 20
Type of magnetic structure (M: magnet; F: focusing lens; D: defocusing gap; O: free gap)	MOFODOFOMO
Number of periods of magnetic structure	XII
Radius of orbit in bending magnet, m	5.73
Perimeter of orbit, m	96.16
Critical energy (kinetic), GeV	2.55

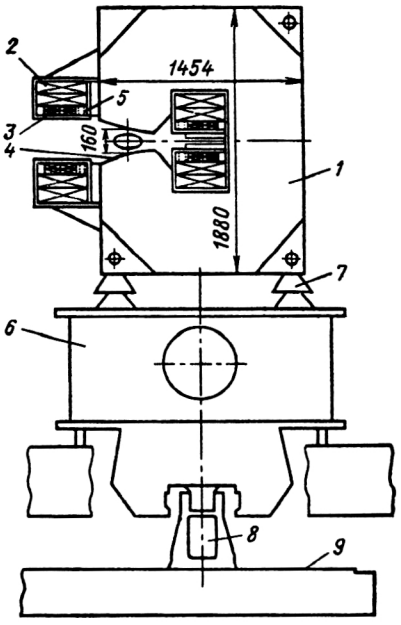

FIG. 18. Cross section of magnetic block of the IHEP synchrotron: 1) magnet circuit; 2) section of main coil; 3) additional coil; 4) pole coil; 5) insulated conductors; 6) carrying beam; 7) packet regulation mechanisms; 8) block regulation mechanisms; 9) foundation slab.

3. THE 70-GeV ACCELERATOR AT THE IHEP

The main IHEP accelerator, the 70-GeV synchrotron, is the largest accelerator in the country. The idea of building such an accelerator was first advanced in 1956 by Vladimirskiĭ, Komar, and Mints and was supported by leading physicists in the country. In 1958, the government of the USSR decided to build the accelerator complex, and in 1961 work on construction commenced at Protvino. Because experience with developing such machines had not yet been obtained in the USSR, a decision was taken to build at the Institute of Theoretical and Experimental Physics in Moscow the first strongly focusing accelerator to 7 GeV in the country, the aim being to test on it the technical decisions adopted for the Serpukhov accelerator. This accelerator was commissioned in October 1961. The physical commissioning of the IHEP synchrotron, at that time the largest in the world, occurred on October 14, 1967.

The Serpukhov accelerator is built in an underground concrete ring tunnel of section 8.4×8.4 m. To reduce the radiation level at the position, there is an additional shielding in the form of an earth mound of the tunnel with a height of about 5 m. Part of the accelerator ring passes through an experimental hall, where protons are extracted from the accelerator together with beams of secondary particles from internal targets of the accelerator.

The magnetic system of the accelerator

The IHEP synchrotron has a magnetic system[34] in which the functions of deflecting the particles in the orbit and the focusing functions are combined in a single magnetic block of C shape. The quadrupole component of the field is formed by the geometry of the profile of the magnetic circuit, which has the form of a hyperbola in the region of the opening of the vacuum chamber. Near the edges of the opening, to reduce the distortions of the magnetic field by edge effects, the profile of the magnetic circuit has correcting projections. This made it possible to create a constancy of the field gradient at a level 0.4% of the rms deviation within 240 mm of the opening at inductances 1.2 T.

The periodic sequence of focusing (F) and defocusing (D) elements, and also free straight sections (O) between the magnetic blocks produces a period of the magnetic structure of the type FODO.

In order to fit equipment into the individual straight sections, some magnetic blocks are shortened, and this leads to a formation of a superperiod of the magnetic structure, which consists of six ordinary magnetic blocks and four shortened ones. Altogether, the magnetic structure consists of 12 superperiods. A magnetic block (Fig. 18) is made from steel plate 2-mm thick of the mark É1 with coercive force 1.5 Oe. The main coil of the electromagnet is made from an aluminum busbar with section 35×72 mm with an opening of diameter 20 mm for water cooling. The busbar length is taken equal to 200 mm to avoid welded connections within a section. The coil consists of four sections, with two in the upper and two in the lower poles. All sections of the same poles are connected in series as regards the current and in parallel as regards the water cooling. The flow of water is monitored by hydrocontacts, the pressure by manometers, and the heating of the water by thermal signals. The coils are cooled by desalinated water with

high electrical resistivity flowing in a closed circuit that includes systems for purifying and cooling the water.

At the present time, coils of two types are used in the correcting circuits (Ref. 35): additional coils surrounding each pole of the block of the electromagnet, and pole coils situated directly on the surfaces of the poles of the magnetic circuit (Fig. 18). The pole coils are in all blocks except block No. 6, where the beam is injected into the ring and there is a larger vacuum chamber. The pole coils are constructed from copper rods of diameter 7 mm insulated from each other and from the frame and placed on the pole surface along the axis. From the 31 rods on each pole several correcting coils of different purposes can be used simultaneously. The additional coils are situated next to the main ones and are made of a conductor with cross section 80 mm^2. On each block there are four additional coils, each with eight windings.

The magnetic-field correction systems of the accelerator make it possible to regulate during the entire acceleration cycle the shape of the equilibrium orbit in the horizontal and vertical, the frequencies of the betatron oscillations, the nonlinearity of the magnetic field, and other parameters. The vertical component of the magnetic field is corrected by means of the additional coils. The gradient, mean plane, and nonlinearity of the field are corrected by the pole coils. In individual blocks, it is necessary to use appreciable correcting magnetic fields, for example, at the positions of beam injection and extraction, where there are thick-wall vacuum chambers with enlarged openings. The eddy currents in the walls of such chambers produce distortions of the magnetic field at the level 2–3%.

The design frequencies of the betatron oscillations in the U-70 accelerator are $Q_r \approx Q_z \approx 9.85$ oscillations with respect to the corresponding coordinate during one period of revolution of a particle in the ring. Various perturbing factors that act on the particles and contain harmonics with frequencies in a definite relationship to the frequencies of the betatron oscillations may lead to resonant growth of the betatron oscillations and, accordingly, to loss of particles. Moreover, during the acceleration process the frequency of the uncorrected betatron oscillations changes, since it depends on the beam intensity and emittance, the particle velocity, and other factors.[36] Because of this, the betatron frequencies, varying during the acceleration period, may pass through several values corresponding to resonance, occupying moreover a definite frequency band. To reduce the influence of these effects, the frequency of the betatron oscillations is stabilized by correcting the magnetic field. The correction of the resonance bands[37] consists of the introduction of additional magnetic fields that excite a field harmonic with definite amplitude (current in the coils) and phase (number of the blocks). In addition, particle loss on the passing of certain types of resonances is reduced by reducing directly the resonance width by switching on correcting coils in a definite scheme.[38–40] The parameters of the resonances are corrected using the varying level of particle loss when the working point of the frequencies of the betatron oscillations in the beam in the accelerator crosses the resonance bands. All the correction circuits are powered from regulated sources, the reference voltages for which are established by means of function generators controlled by a computer.[41] This arrangement of the power-supply control system makes it possible to introduce a dynamic correction during the acceleration cycle and also to use a complicated algorithm for controlling the correcting currents that ensures independent regulation of the individual resonance bands.

The basic parameters of the magnetic system of the IHEP synchrotron are as follows:

Number of blocks of electromagnet	120
Number of superperiods	12
Structure of magnetic period	FODO
Number of blocks of normal length:	
focusing	36
defocusing	36
Length of block in iron, m	10.42
Mass of block, ton	216
Number of shortened blocks:	
focusing	24
defocusing	24
Length of shortened block, m	9.3
Mass of shortened block, ton	197
Total mass of active steel, ton	19 500
Total mass of aluminum of main coil, ton	550
Radius of curvature in magnetic block, m	194.125
Length of equilibrium orbit, m	1483.7
Mean radius of orbit, m	236.2
Opening of vacuum chamber ($r \times z$), m	0.17×0.115
Induction at injection of 1.5-GeV beam, T	0.0386
Induction in equilibrium orbit at energy 70 GeV, T	1.2
Relative gradient of magnetic field, m^{-1}	2.35
Nominal rate of growth of magnetic field, T/sec	0.41

Power-supply system of ring electromagnet

The magnets of the U-70 accelerator are powered through regulated thyristor transformers from main power systems, each of which consists of an asynchronous motor of power 7 MW, a synchronous generator, a 54-ton flywheel, an auxiliary generator that controls thyristor rectifiers, and a machine slip regulator. The rotor of the synchronous generator is set in rotation by the asynchronous motor with flywheel on a single shaft. The flywheel possesses appreciable kinetic energy and is used to accumulate

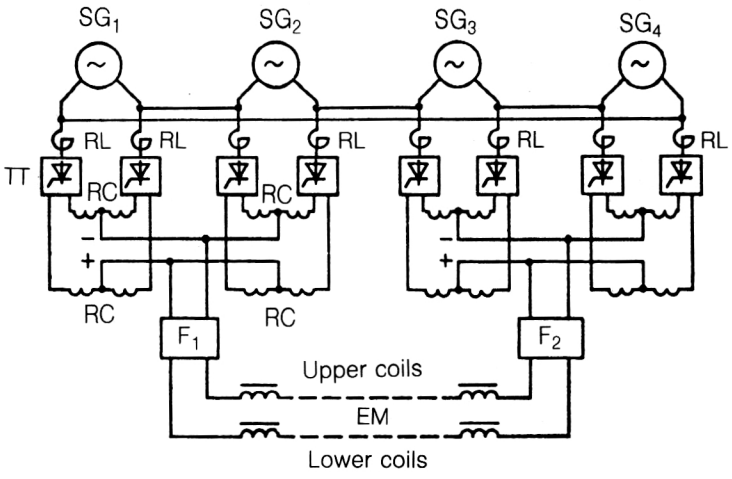

FIG. 19. Schematic representation of power supply of the coils of the ring electromagnet: TT are thyristor transformers; SG are synchronous generators; DC are dividing coils; RL are linear current-limiting reactors; F1 and F2 are filters; EM are coils of the electromagnet.

energy between the pulse load and the energy system. The maximal power of the generator in a pulse is 34 MW, and the maximal total required pulsed power in the ring magnet is about 80 MW. The energy exchange in a cycle is due to transformation of the kinetic energy of the systems into energy of the magnetic field and back again; the motors are designed only to cover the mean losses in the equipment. The mean active power required from the grid is approximately 15 MW, the remaining power being covered by the stored kinetic energy of the flywheel.

The power supply of the ring magnet is shown in schematic form in Fig. 19. It contains four synchronous generators SG and bridge thyristor transformers TT.[42] Synchronous operation of the generators is ensured by connection of their coils by synchronizing circuits in a circular scheme. To maintain equality of the currents in the coils of the electromagnets, a regime of successive powering of the circuits of the upper and lower coils of the electromagnet is used.[43] The sources are connected in series in a single current circuit of the electromagnet ring. To reduce the amplitude of the harmonics in the rectified voltage a 12-phase rectification scheme is used in the circuit of both power sources. It consists of two bridges connected in parallel through dividing coils DC. Each pair of bridges is powered from a synchronous generator, the two isolated starting coils of which are put together in two "stars" with displacement of 30 electric degrees relative to each other. Each power source consists of two such circuits connected in parallel.

To ensure a high stability of the flat part of the magnetic-field pulse, which is needed to operate the systems for slow extraction of the proton beam from the accelerator, the power supply includes passive filters F and a system of automatic regulation of the firing angles of the thyristor transformers if the magnetic field at the top of the pulse deviates from the prescribed value.[44] The achieved level to which the nonuniformity of the field is reduced in the flat part of the pulse is not worse than 5×10^{-5}.

Figure 20 shows a cycle of operation of the electromagnet. The thyristor transformer operates in the rectifying regime at the level 386 Oe, where the intermediate flat part of the pulse with duration of about 2 sec and field stability $\pm 2 \times 10^{-4}$ is formed for the injection of the particles from the booster.[45] The field is then raised to the level 1.2 T (beam energy 70 GeV), and at this level field stabilization is maintained for 2 sec, during which the fast and slow beam extractions are made, and the beam is also directed onto internal targets of the accelerator. During the field decay, the thyristor transformer is switched to the inverter regime for 2.8 sec, during which time the synchronous generator works as a motor powered by the energy stored in the magnet, this being transformed into kinetic energy of the flywheel. The duration of one cycle in the working regime is ~9.5 sec.

The characteristics of the electrical supply system of the ring electromagnet are as follows:

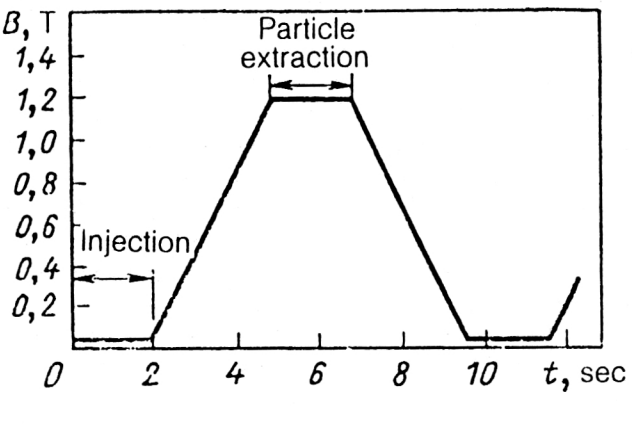

FIG. 20. Cycle of variation of the magnetic field of the ring electromagnet of the accelerator.

Total maximal voltage in circuit powering the coils of the electromagnet, V	16 200
Current in coil at induction 1.2 T, A	4800
Maximal employed pulsed power in the electromagnet, MW	80
Mean power required by the power-supply system from the grid, MW	About 15
Stored energy in ring electromagnet for field 1.2 T, MJ	About 73

Accelerating system of the synchrotron

The complex of the accelerating system consists of a master oscillator with frequency programmed to vary in the range 5.56–6.1 MHz, amplifiers of the rf signal, and 40 accelerating stations. The master oscillator ensures the necessary functional dependence of the frequency of the rf signal on the magnetic field and corrects the frequency using data on the radial position of the centroid of the bunches of accelerated particles and the equilibrium phase of the accelerating field. The required dependence of the frequency on the magnetic field strength is formed by a functional converter, whose input receives a signal from an induction coil placed in a gap of a separately situated measuring magnet analogous to the electromagnetic blocks in the ring of the accelerator and connected in the power-supply circuit in series with them. The deviation of the bunch centroids from the prescribed radial position and from the equilibrium phase is recorded by electrostatic electrodes set up in the vacuum chamber of the accelerator. Signals from the sensors are analyzed by an appropriate electronic circuit, from the output of which a control voltage is sent to the input of the master oscillator. Each station consists of a preamplifier of the rf signal and a high-power two-cascade tube amplifier and accelerating resonator (Fig. 21) positioned in straight sections of the accelerator.[46] The power sources, amplifiers, and parameter control blocks are in five service radio-apparatus halls; the central control apparatus and station control are in the accelerator control hall. The resonator consists of two coaxial short-circuited lines excited in antiphase (Fig. 21b). The common gap ensures a strong capacitance coupling of the two resonance circuits, each of which is surrounded by ferrite cores of the mark 300NN. The resonance frequency of the cavity is tuned by changing the magnetization current of the ferrite. To screen the beam from stray fields of the magnetization coil, the inner tube of the resonator is made of magnetically soft steel and is part of the vacuum circuit. The inner tube in the accelerating gap has an insulating partition made of ceramic. The accelerating stations are equipped with systems of autoregulation of the amplitude and frequency self-tuning. The reference voltage for the amplitude autoregulation system is shaped in the form of a piecewise broken curve by a function generator common to all the stations and is transmitted to the accelerating stations in digital form. The accuracy with which the

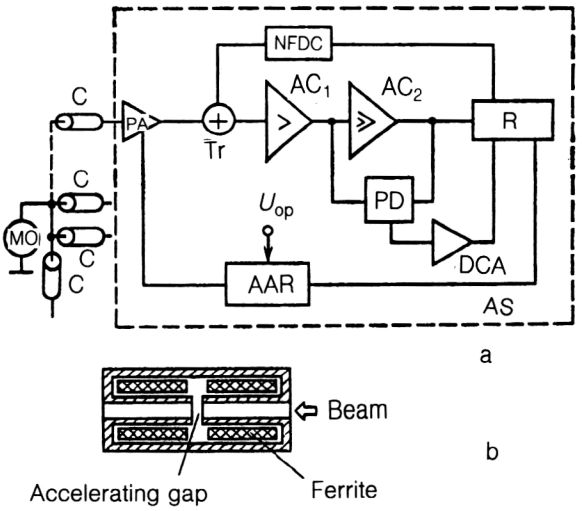

FIG. 21. Simplified block diagram of accelerating system of the U-70 synchrotron (a) and sketch of accelerating resonator (b): AS is an accelerating station; MO is the master oscillator; C is a cable; PA is a preamplifier; Tr is a summing transformer; AC_1 and AC_2 are high-power amplifier cascades; NFBC is the negative feedback circuit; R is the resonator; PD is the phase discriminator; BCA is the dc amplifier; AAR is the automatic amplitude-regulation circuit.

prescribed law of variation of the amplitude is followed is ±5%. In the frequency self-tuning system, the reference phase is the phase of an rf voltage in the grid of the tube of the final cascade. The phases of the accelerating and reference voltages are compared by means of a phase discriminator. The error signal from the discriminator is amplified and used as a control signal of the rectifier that powers the magnetization coils of the ferrite. The bunched beam induces in the accelerating resonator an rf voltage, which is added to the voltage produced by the rf oscillator. The resultant rf voltage in the resonator becomes dependent on the amplitude and phase of the beam current. In such a situation, the autoregulation systems can go over to a regime of unstable fluctuations. To weaken the coupling of the resonator to the beam, a negative feedback with respect to the high frequency is used.[47] This covers both cascades of the final high-power amplifier (Fig. 21a). Each accelerating station produces an accelerating voltage up to 10 kV. For nominal total voltage 360 kV, four stations remain in reserve. In the injection regime, the required total accelerating voltage is 120 kV, and is ensured by lowering the accelerating voltage in each station to 3.3 kV. On the transition from the injection regime to the acceleration regime, the voltage is increased to the nominal value during 50 msec. Each station is controlled by a block that controls the amplitude and phase of the output voltage. In addition, some further important parameters are controlled by local elements of the electronics. The cable communications for these elements are connected to a computer, by means of which the parameters are periodically monitored.

The main parameters of the accelerating system of the U-70 are as follows:

Number of accelerating stations	40
Amplitude of accelerating voltage in resonator, kV	10
Range of variation of frequencies during operation with booster, MHz	5.56–6.1
Maximal rate of change of frequency, MHz/sec	About 140
Maximal rf power, kW	30
Maximal power required by a station, kVA	80
Maximal power of loss in ferrite, KW	10
Maximal magnetization current of ferrite, A	95
Length of resonator, mm	1350

Vacuum system of the accelerator

In accordance with the requirements on the beam, the pressure of the gases in the ring chamber of the U-70 synchrotron must not exceed the level 1.3×10^{-4} Pa (10^{-6} mm Hg). The reason for the restriction is the same here as in the ring injector booster. One of the main elements of the ring vacuum system[48] of the U-70 accelerator is a vacuum chamber of length 11 m in the gap of a magnetic block. It is a corrugated tube of elliptical section with internal dimensions 115×200 mm and wall of thickness 0.4 mm, which is made of stainless steel of the mark 12Kh18N10T. To limit the eddy currents induced in the wall of the chamber by the magnetic field, an electrically insulating insertion is built in at one of the ends of the chamber in order to separate the chamber electrically from the remaining ring. In addition, the magnetic circuit of the block is also insulated from the vacuum chamber by special insertions. The chamber is electrically grounded to eliminate the static charge formed when protons lost from the beam in the acceleration process impinge on the walls. There are special smooth-wall vacuum chambers with wider openings at the sections of beam injection and extraction.

The vacuum chamber of the accelerating station is part of the construction of the cylindrical resonator—its inner tube. It is a corrugated oval tube with inner dimensions 105×185 mm, length 1490 mm, and accelerating gap in the center insulated by a ceramic insertion of the mark 22KhS. Between the connecting collars and the vacuum chamber itself there are sylphon bellows to eliminate mechanical loads on the resonator chamber. Besides the accelerating stations the straight sections have vacuum boxes of instruments for observing the beam, boxes of magnets for injecting and extracting the beam, etc. The elements of the ring vacuum chamber are connected by bolted flanges. Vacuum sealing of the flanges is ensured by metal washers. In some places, this is done by means of washers made of vacuum resin, which simultaneously fulfill the role of electrical insulation. To separate the vacuum regions when repair work is being done on equipment, and also to insulate sections if there is a local breakdown of the vacuum sealing, sliding shutters of pendulum type are used. Beams are extracted from the accelerator in the region of experimental facilities at several positions along corresponding directions. Because the required level of the vacuum in the beam transportation channels is about 10^{-2} mm Hg, the high-vacuum system of the accelerator is separated from the vacuum regions of the channels by thin metallic barriers, which are made of titanium of thickness 50 μm, stainless steel (100 μm), or aluminum (300 μm).

The vacuum regions of the ring chamber of the U-70 are evacuated in a three-stage process. Forevacuum VN-1 pumps are used down to pressures of about 5×10^{-2} mm Hg. The evacuation in the range 10^{-2}–10^{-5} mm Hg is done by means of preliminary vacuum stations of two types, consisting either of an NVZ-20 mechanical pump and a TMN-500 turbomolecular pump or a VN-2 pump and a VA-0.5 vacuum system. In the following range of pressures, from 10^{-5} mm Hg to the working pressures 10^{-6}–10^{-7} mm Hg, magnetic-discharge pumps of the type NÉM-300 or NMD-0.4 are switched on.

For convenience of operation, the vacuum ring chamber is divided into 20 sections, at the boundaries of which there are vacuum shutters. Each section has a VN-1 forevacuum pump, a preliminary vacuum station, and five or six titanium magnetic-discharge pumps. In the straight sections containing the bump magnets, septum magnets, and beam-diagnosis systems, enhanced gas release is observed, and therefore additional titanium pumps are installed in these sections. At the present time, between 138 and 144 magnetic-discharge pumps work simultaneously in the vacuum ring system. The level of the vacuum in the working regime is controlled in each section by means of the current level of the magnetic-discharge pump. The accelerator systems are protected from deterioration of the vacuum by means of MM-15 vacuum sensors and vacuum blocking systems.[49] If the pressure rises above the level 2×10^{-4} mm Hg, the accelerating stations are automatically switched off, the opening of the channel for injecting the beam into the U-70 accelerator is closed by a beam shutter (beam absorber), and the defective section is separated from the remaining part of the vacuum ring chamber by sliding shutters. The vacuum system of the U-70 is controlled both from the main panel of the accelerator and from local panels in the ring tunnel of the accelerator. A mean working level of the vacuum of about 8×10^{-5} Pa ($\sim 6 \times 10^{-7}$ mm Hg) can be maintained in the ring chamber for a long continuous run of the accelerator (30–40 days).

Systems for suppressing beam instability

During the acceleration process, there are losses of the beam and an increase of its dimensions, not only due to resonance betatron oscillations but also through the occurrence of beam instabilities due to space-charge effects, which lead to the appearance of coherent betatron oscillations with growing amplitude. These instabilities appear at beam intensities above certain threshold values and are due to interaction of the current of the particles of the beam

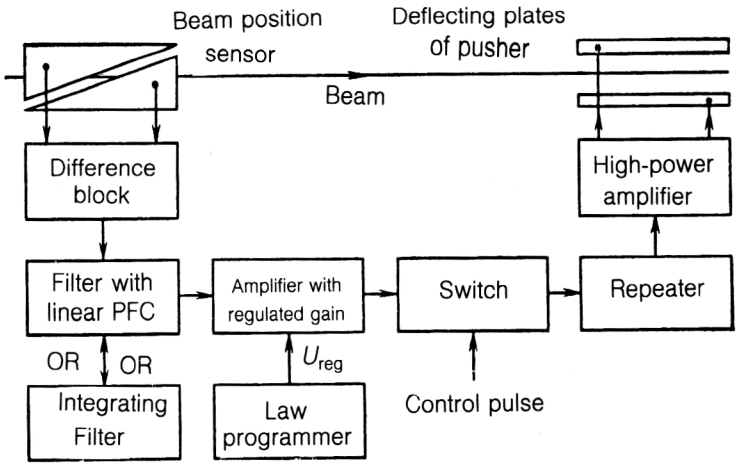

FIG. 22. Block diagram of narrow-band system for suppression of coherent betatron oscillations. PFC denotes phase-frequency characteristic.

with the electromagnetic fields that arise in the region bounded by the conducting walls of the vacuum chamber or resonant elements of the equipment surrounding the beam. A resistive wall instability is due to the finite conductivity of the chamber walls. The beam of charged particles, executing betatron oscillations around the equilibrium orbit, induces an electric image current of the beam in the conducting wall of the vacuum chamber. The electromagnetic field of the beam image, in its turn, acts on the oscillating beam, and if there are certain phase relations between the electromagnetic field of the beam and the image field, then the beam oscillations will grow. Growth of coherent instability of the beam can be prevented by the method of introducing a spread of frequencies into the betatron oscillations of the beam. This method is based on the dependence of the frequencies on the radius of the instantaneous orbit and on the amplitude of the betatron oscillations when quadratic and cubic nonlinearities of the magnetic field are introduced. To this end, sextupole and octupole lenses are included in the ring; their use raises the threshold of the stable state of the particle ensemble. However, the increase in the spread of the betatron frequencies can cause frequencies to enter the bands of betatron resonances, and therefore a radical way to overcome these difficulties is to use electronic systems to suppress the coherent oscillations. In the general case, a system of this kind consists of beam position sensors, electronic blocks that separate the useful signal and form definite phase relations, and executing devices that act on the beam (beam dampers).The main characteristics of the suppression systems are the frequency range of the feedback circuit and the decay rate introduced by the system into the beam oscillations. Narrow-band systems act on one or several excited harmonics of the smooth beam and its collective oscillations of the bunches. The wide-band systems act not only on the collective oscillations but also on the oscillations of the individual bunches that are not related to each other or on parts of one bunch. The existence of uncoupled oscillations of the bunches is explained by the fact that, physically, a bunch of particles can be represented as an oscillator for which the coherent frequency of oscillations depends on the number of particles in it. A spread of the bunch intensities (or appreciable modulation of the intensity over the length of a bunch) leads to a spread of the coherent frequencies of the bunches (respectively, within a bunch). If this spread is appreciable, the reflected electromagnetic field in the walls of the vacuum chamber cannot couple the oscillations of the bunches to each other.

In the IHEP accelerator use was made for the first time of the principle of a double feedback circuit.[50] Two circuits, which are not instrumentally coupled, simultaneously suppress the betatron oscillations of the beam. A narrow-band feedback introduces appreciable decay rates into the low-frequency (8–12) harmonics of collective oscillations of the beam. The wide-band feedback ensures suppression of the uncoupled oscillations of the bunches.

Besides the direct functions of suppressing the coherent beam oscillations, such systems are used in the IHEP accelerator for diagnosis of the transverse motion. The time of development of the instabilities is measured by breaking the feedback circuit at intensities above the threshold level. The frequencies of the betatron oscillations are measured by pulsed excitation of the beam by a pusher synchronously with the breaking of the circuit,[51] or by exciting the beam by a bump magnet of the extraction systems.

The narrow-band system (Fig. 22)[52] has two independent channels for the r and z directions. For effective suppression of the instabilities in the different regimes of operation of the accelerator, the necessary phase and frequency characteristics of the narrow-band system are realized by switching parallel circuits, which have the characteristic of an integrating link and a linear phase characteristic. The required dependence of the gain in the acceleration cycle is ensured by a law programmer. The final amplifier, the load of which is the deflecting plates of the electrostatic beam pusher, develops a voltage with amplitude up to 3.5 kV. The resulting frequency range of the feedback circuit is 1–350 kHZ.

The wide-band system[53] for suppression of coherent oscillations also consists of two independent channels for the r and z directions, each of which includes two electrostatic sensors of the beam position, a magnetic beam exciter, and an electronic circuit for shaping the feedback

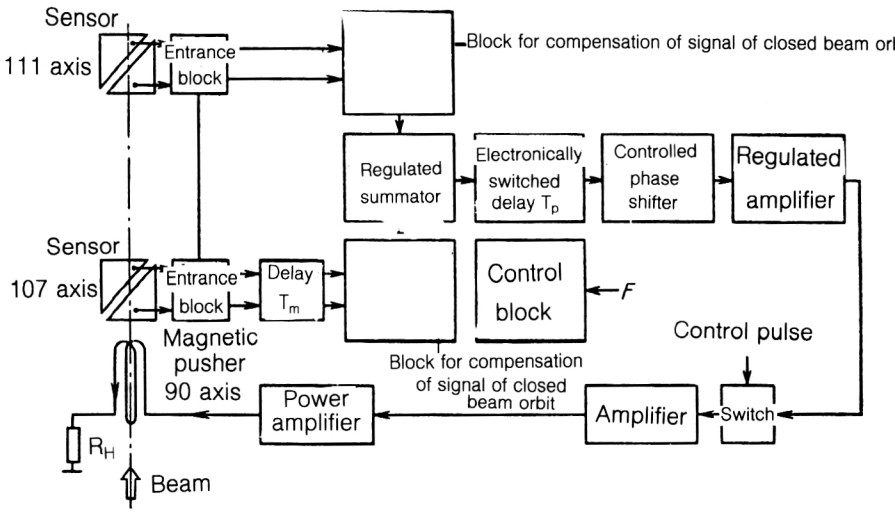

FIG. 23. Block diagram of wide-band system for suppressing coherent betatron oscillations.

signal (Fig. 23). The voltages from the plates of the electrostatic sensor are modulated by signals that carry information about both the coherent oscillations of the individual bunches and the low-frequency oscillations of the closed orbit of the beam. The betatron frequency of the beam is about two orders of magnitude higher than the frequency of the low-frequency oscillations of the beam orbit. To ensure the required dynamic range of operation of the system at the high frequencies, it is necessary to eliminate the low-frequency modulation of the signals coming from the electrostatic sensors by means of a compensation block. The maximal decay rate introduced by the suppression system into the betatron oscillations of the beam is attained when the position sensor and beam pusher are placed at points in the accelerator separated by an odd number of quarter-wavelengths of the betatron oscillations. To meet this condition for all working frequencies, it is sufficient to position two sensors at different azimuths of the accelerator and add the signals with definite weight coefficients. By varying the values of these coefficients, one can create a virtual sensor displaced in azimuth by the required distance from the beam pusher. The signals are added by a controlled summation device. The feedback circuit includes an electronically controlled delay line, which is used to maintain equality between the bunch flight time and the time of signal propagation from the sensor to the pusher as the beam velocity changes during the acceleration process. The delay control block is synchronized with the frequency of the accelerating field. A high-power output amplifier connected to the magnetic pusher ensures a maximal output current up to 6 A. With allowance for all the frequency characteristics of the circuits, the resultant working band of frequencies of the system is 0.2–10 MHz.

The use of the wide-band system facilitated a series of investigations on the dynamics of the circulating beam in the regime of injection from the booster. The combined use of the narrow- and wide-band systems for suppressing the coherent betatron oscillations permitted operation of the IHEP accelerator with a beam intensity of about 1.6×10^{13} protons in a cycle.

Beam instabilities leading to particle losses are also associated with longitudinal oscillations of the particles around the equilibrium (synchronous) phase of the accelerating field.

Instability of longitudinal oscillations is observed in the U-70 accelerator when a critical energy (about 8.9 GeV) is passed during the acceleration cycle. As a parameter, this energy is characteristic only for the strongly focusing magnetic structures of the accelerator and is associated with the abrupt change of the conditions of the periodic longitudinal oscillations. At an energy of the particles below the critical value, the stable equilibrium phase is situated in the rising part of the sinusoid of the rf voltage ($-\varphi_s$), while at an energy above the critical value it is abruptly shifted to the descending part, taking the value $+\varphi_s$. To match the particle trapping regimes below and above the critical energy, a method of rapid switching of the phase of the rf oscillations by $2\varphi_s$ is used. The development of the longitudinal instability of the beam in the IHEP accelerator was noted through a sharp rise in the longitudinal phase space of the bunches after crossing of the critical energy.[54] The development of the instability is accompanied by microwave modulation of the beam current in the range of frequencies 6 GHz and a loss of beam intensity due to ejection of some of the particles from the stability region with increased pulsed spreading of the particles.[55] There are several versions of the physical reasons for the development of this beam instability.[55–58] According to the investigations of Ref. 58, at a beam intensity of about 10^{12} protons/cycle microwave radiation appears about 5–10 msec before the critical energy, increases smoothly in the subcritical region, and gives an abrupt burst 2–3 msec after the critical energy. At the same time, the occurrence of the instability depends only on the number of particles in a bunch ($\sim N_{cr} > 10^{10}$ particles) but not on the number of bunches. The reason for the instability is the effect of the microwave field induced by the beam in the cavity of the vacuum chamber. The experimental dependences of the beam modulation frequency and the rf impedance of the coupling of the vacuum chamber lead to an explanation of these data by the representation of the vacuum chamber as a decelerating structure like a stopped

waveguide, where the corrugations of the chamber play the role of the stops. Such a representation was investigated both theoretically[59] and experimentally.[58] The microwave propagates with phase velocity close to the velocity of the particles and interacts with a bunch. The microwave disturbance generated by the "head" of a bunch excites its "tail" but is not transmitted further to the following bunches because of the rapid damping of the field.[60] The effect of the microwave field is merely to rearrange the particles in the longitudinal direction relative to the distribution satisfying the equilibrium state. The occurrence of the instability is due to the fact that in the region of the critical energy the beam is compressed in the longitudinal direction about the equilibrium phase, and this corresponds to a rise in the local density of the beam and leads to the onset of the instability. The process has a threshold nature with respect to the charge density of the bunch and develops without an initiating situation, in which it also differs from an ordinary instability. The investigations show that to ensure operation of the U-70 with intensity 5×10^{13} protons/cycle it is necessary to reduce the high-frequency impedance of the coupling of the vacuum chamber of the accelerator and to use a rapid passage through the critical energy in the acceleration cycle.[61] An increase in the rate of change of a parameter in a region dangerous for beam stability is a characteristic method in accelerator technology. In the IHEP accelerator, this is achieved by a system for jumping the critical energy,[62] by means of which the gradient of the magnetic field is perturbed in two radially focusing blocks of the electromagnet in each superperiod of the accelerator. The frequency of the azimuthal harmonic of the perturbation introduced in this manner is close to the frequency of the 12th harmonic of the radial betatron oscillations. The shift of the critical energy corresponds to the perturbation introduced in the magnetic field. The principle of operation of the system is as follows. At an energy of the particles close to the natural critical energy, a comparatively slow anticipatory increase of the critical energy of the accelerator is initiated. As the beam energy approaches the new critical value, the power sources are switched off at the time of arrival of the synchronizing pulse, and the critical energy returns to the original value as the current falls rapidly in the correcting coils. In the operating system,[57] the passage of the beam through the critical energy is accelerated by about 30 times. The coils powered by this system belong to the circuit that corrects the gradient of the magnetic field of the accelerator. There are 24 independent sources[63] that produce triangular current pulses with rise time of about 30 msec, decay time of about 0.75 msec, and maximal amplitude of about 80 A. As was noted above, transition through the critical energy requires matching of the phase spaces of the beam at the new equilibrium phase of the rf accelerating voltage. The phase is switched by a programmable computer in the frequency self-tuning circuit of the accelerating stations. Considered overall, the system for carrying the beam through the critical energy is an effective means for reducing the particle loss. The jump of the critical energy eliminates the burst of the longitudinal beam instability in the local region of the critical energy and thus makes it possible to maintain the intensity of the particles in the acceleration cycles.

Main parameters of the U-70 synchrotron

Energy of accelerated protons, GeV:	
maximal	76
working	70
Intensity:	
design, proton/cycle	5×10^{13}
achieved by December 1988, proton/cycle	1.6×10^{13}
Cycle repetition period, sec	9.5
Frequency of accelerating voltage, MHz	5.56–6.1
Critical energy, GeV	About 8.9
Mean radius of orbit, m	About 236

4. BEAM EXTRACTION SYSTEMS

The extraction of the beam from the accelerator and formation of the beam with the parameters needed for the physics experiments are among the most complicated problems in accelerator practice. Up to now, four methods of beam extraction have been developed for the IHEP accelerator. Each of them covers a certain range of energies and intensities of the extracted beams. Historically, beam extraction from internal targets was the first method that permitted physics experiments in a wide range of energies of secondary particles from 10 to 60 GeV and designed for fluxes of the secondary particles up to 10^7 particles/cycle. Nonresonant slow extraction of protons elastically scattered by an internal target was developed in recent years in order to meet the need for beams with intensity 10^6–10^{10} protons/cycle. Rapid extraction was formulated as a method to meet the requirements of experiments with bubble chambers, in which a beam of protons is directed onto an external target with energy around 70 GeV, intensity 10^{11}–10^{13} protons/cycle, and extraction duration up to 5 μsec. Finally, slow extraction provides high-intensity beams of 10^{10}–10^{13} protons/cycle with an energy of about 70 GeV for experiments by the electronic method with the extraction of the particles lasting up to 1 sec. The sequence of operation of the extraction systems is as follows. At the end of the acceleration cycle, rapid extraction of a bunched beam can be carried out; then, after debunching of the beam in the flat part of the magnetic cycle there can be slow extraction or extraction of particles from internal targets, or these methods can be used in succession.

Extraction of particles from internal targets

In the IHEP accelerator, the method of obtaining beams of secondary particles from internal targets[64] is realized as follows. On completion of the acceleration of the particles to the final energy, the proton beam is shifted radially (± 5 cm) from the central orbit by means of magnetic systems that produce a local distortion of the orbit

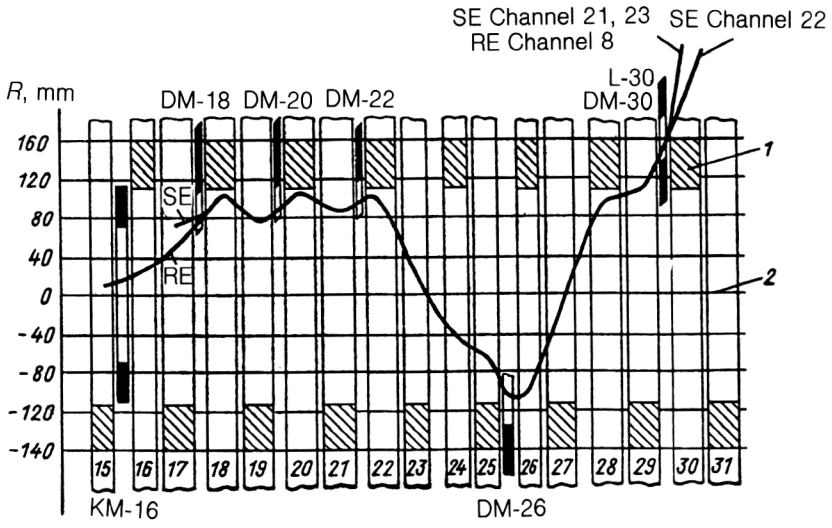

FIG. 24. Schemes of systems of rapid and slow extraction of the beam from the U-70 accelerator: 1) region of strong nonlinearity of the magnetic field; 2) center of vacuum chamber of accelerator; KM is the rapid-extraction kicker magnet; DM are deflecting septum magnets; L is a quadrupole lens; SE is slow extraction; RE is rapid extraction.

(bump). Before this, a target, fixed to a support, is introduced in the region of the local disturbance. Some of the particles produced on the target pass through the magnetic field of the accelerator and can be formed into a beam by the following magneto-optical system of the transporting channel. By a slow increase in the amplitude of the local perturbation, the remaining beam of protons is guided in the subsequent revolutions onto the target,[65] thus ensuring a duration of the beam of secondary particles up to 2 sec. By means of this method, the IHEP accelerator can be operated simultaneously with up to three targets[66] in the magnetic blocks Nos. 24, 27, 33, and 35 of the accelerator and in the 36th straight section. The momentum of the particles collected into the channel depends on the radial position of the target relative to the optic axis of the channel, since the field of the electromagnet of the accelerator plays the part of a preliminary magnetic analyzer. The size and material of the target are chosen on the basis of the required efficiency of interaction of the accelerated beam with the target and the parameters of the transporting channel. Targets made of light metals are most often used, the reason for which is that as a result of multiple passage of the beam through a target the dimensions of the primary proton beam are increased more strongly by Coulomb scattering processes, the heavier the matter of the target.[67] Targets made of beryllium and aluminum, which have high relative yields of secondary hadrons, are widely used. In the case of slow guiding of the beam onto a target, beams that are sufficiently uniform in time and elimination of the modulation that arises from the influence of the instabilities of the beam parameters in the accelerator and the pulsations of the current in the power sources of the magnetic systems can be achieved only by introducing into the guiding system a feedback with respect to the current of particles from the target.[65] A signal from the sensor of the beam current from the target is sent to a circuit[68] that controls the currents in the additional coils of the magnetic blocks of the accelerator that produce the perturbation of the orbit. The feedback closed in this way maintains the intensity of the extracted beam in the case of operation with one target with fluctuations at the level 10–20%. If two or more targets are operated, the fluctuations of the beam intensity are, as a rule, larger. However, by using thin targets (about 50 mg/cm^2), one can obtain better results and ensure modulation of the intensity at the level 7–10%.[69] The frequency range of the system makes it possible to treat intensity fluctuations in a frequency band up to several hundred Hz. For effective use of the duration of the flat part of the magnetic cycle of the accelerator, one can use successive operation of targets with different bumps. In this regime, the dead time is largely determined by the rise time of the current in the additional coils of the blocks (about 0.15 sec).

Among the advantages of this method of beam extraction one must include the high efficiency of interaction of the accelerated beam with the target (about 90%), and also the comparative ease with which beams of secondary particles extended in time can be obtained. However, with increasing intensity of the primary beam on the target (more than 10^{12} protons/cycle), the problem of activating the accelerator equipment becomes very serious. Therefore, the main method of using high-intensity beams is to extract them from the accelerator with high efficiency and to generate secondary particles on external targets.[70]

Rapid extraction of protons from the accelerator

This method is based on extraction of one or several bunches of the beam by a powerful pulsed magnet (kicker magnet) in a straight section of the accelerator, with the growth and decay of the field in the magnet taking place in the time interval between the passage of neighboring bunches of the beam. Having received an angular deflection in the kicker magnet (KM-16), the proton beam passes through deflecting septum magnets (DM), which are common to the rapid and slow beam extraction methods (Fig. 24). To shift the beam into the opening of the deflecting magnets, an additional perturbation of the beam orbit (a bump) is created by switching on additional coils in the blocks Nos. 15–21 and Nos. 16–22 (block 15 is for

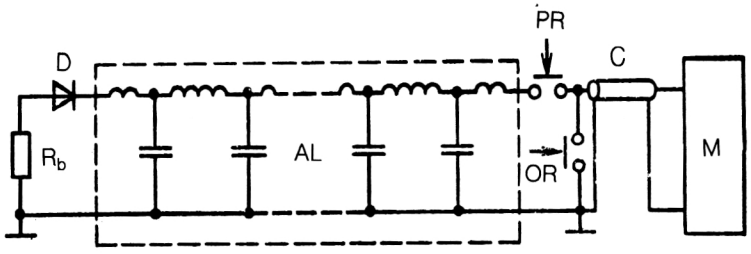

FIG. 25. Circuit of pulsed power supply of kicker magnet: PR, OR are switches; R_b is the ballast load; D is a diode; M is the kicker magnet; AL is an accumulator line; C is a cable.

guiding, 21 for correction, etc.). In a number of cases that extend the possibilities of rapid extraction, a kicker magnet can be used in the 14th section, like KM-16, and also a pulsed magnet DM-24 (not shown in Fig. 24). Depending on the current in the magnet DM-30, the beam is directed either along the track of channel No. 8, or along the track of channel No. 22. The stray magnetic field of the accelerator has a defocusing effect on the extracted beam. To correct this, there is the quadrupole lens L-30, which carries out a preliminary focusing of the beam. The kicker magnet with its power-supply system[71] is one of the most complicated devices in the equipment of the rapid beam extraction. It consists of ten identical modules, each of which is powered by its own pulsed generator. The magnetic circuit is made from C-shaped ferrite cores. The single-winding coil is made in the form of flat busbars, an inner one and an outer one. The current pulse in the coil is formed by discharging to the coil an artificial storage line charged to 70 kV (Fig. 25). Each line has two commutating spark discharges in the working volume of which air under pressure 0.4–0.6 MPa is used. Activation of the switch PR shapes the leading edge of the current pulse in the magnet. The time lag between the firing of this discharger and the switch OR guarantees the necessary duration of the pulse for extracting the required number of bunches. The high-voltage diode D serves to throw the unused energy of the artificial storage line into a matched ballast load. The accuracy of synchronization of the generators of all modules with each other and relative to the phase of the rf voltage of the accelerator is not worse than ± 5 nsec. Extraction of an intense beam imposes special requirements on the reliability of the power supply of the kicker magnet. A feature of the employed high-voltage dischargers is the relatively narrow range of stable operation with respect to individual parameters. Instabilities in the system can lead to missed firings or to spontaneous premature breakdowns of the dischargers in individual modules. This will result in the occurrence of false pulses of the magnetic field with the beam circulating in the accelerator or a decrease of the integrated field of the magnet in a working cycle. As a result of this, the radiation circumstances along the track of the beam extraction may be significantly changed. To eliminate these effects, a system for stabilization of the integrated field was developed.[72] The system, in which a computer is used, controls the operation of the pulsed generators and stabilizes the field by automatically switching on a reserve module of the magnet. The basic parameters of the kicker magnet and its power-supply system are given in Table II. The septum magnets situated further down the extraction track are equipment whose parameters and construction were determined by the more stringent conditions of the systems of slow beam extraction. For this reason, it will be appropriate to consider their construction and parameters when we describe the slow extraction systems. At the present time, rapid beam extraction operates only in one direction, permitting experiments with the facilities Neĭtrino, Neĭtrinnyĭ Detektor, and the bubble chamber SKAT, the beam to which is formed by channel No. 8. As a result of investigations[73] aimed at achieving the projected intensity in the channel of 3×10^{13} protons/cycle, the parameters of the extracted beam are being improved, and for reference we may give the main parameters achieved by 1988: At beam intensity 10^{13} protons/cycle, the extraction efficiency is 95%, the emittance in the horizontal and vertical planes is 2π mm·mrad, the momentum spread is about $\pm 1.5 \times 10^{-3}$ at the 95% intensity level, the number of

TABLE II. Parameters of magnets of the beam extraction system.

Parameter	Type of magnet			
	Kicker magnet KM-16	Septum magnet DM-18	Septum magnet DM-20	DM-22, DM-26
Maximal induction of magnetic field at center of magnet, T	0.1	0.0805	0.75	1.26
Length of magnet in iron, m	3	1.26	1.3	1.3
Angular deflection at energy 70 GeV, mrad	1.02	0.44	4.25	7.18
Excitation current, kA	8	1.6	7.5	8
Opening of magnet $r \times z$, mm	140×100	45×25	48×23	48×28
Current density in septum, A/mm^2	—	128	136	139
Thickness of septum, mm	—	0.5	7.5	13.8
Duration of leading edge of pulse, nsec	160	—	—	—
Duration of trailing edge of pulse, nsec	200	—	—	—

extracted bunches is between 1 and 30, and the maximal intensity of the extracted beam is about 1.6×10^{13} protons/cycle.

Slow proton extraction from the accelerator

The slow extraction system is intended to extract a proton beam with energy from 20 to 70 GeV and projected intensity up to 3×10^{13} protons/cycle for experiments using the counter method.[74] The extraction is done in the flat part of the magnetic cycle of the accelerator, with duration up to 1 sec, in the direction of channel No. 8 and into channel No. 22. The extraction scheme is based on the excitation of radial betatron oscillations at the third-order resonance $3Q_r = 29$, i.e., the frequency of the betatron oscillations is shifted in such a way that the resonance conditions for the betatron oscillations are satisfied in three complete revolutions of the beam, thus leading, in the presence in the accelerator of harmonics of the magnetic field at this frequency, to an appreciable increase in the amplitudes of the radial oscillations of the beam. The resonance has a broad band, and this is of no little importance, since the duration of the extraction is determined by the time of passage through the resonance band.[75] The resonance is excited by introducing the 29th harmonic of the quadratic nonlinearity of the magnetic field by means of four sextupole lenses distributed at intervals of 90° in the accelerator azimuth and in the straight sections Nos. 12, 42, 72, and 102. Two lenses at right angles to each other form the sine and cosine components of the 29th harmonic, and this makes it possible to select the necessary phase of the perturbation at any azimuth of the accelerator. Switching of the lenses along a diameter of the accelerator in opposite polarity compensates the constant component and the even harmonics of the quadratic nonlinearity of the field. The cubic nonlinearity of the magnetic field has an important influence on the development of this resonance. To compensate it, there are two octupole lenses in the straight sections Nos. 34 and 94. The adjustment to resonance ($Q_r = 9.66...$) is achieved by a quadrupole lens in the 38th straight section. The extraction duration is determined by the rate of change of the gradient in the lens. The required rate of change of the frequency of the betatron oscillations on the passage through the resonance band is very small. Parasitic pulsations in the magnetic fields of the accelerator or in the lenses of the system that excites the betatron oscillations will give rise to a density modulation of the beam. In this connection, the requirement of uniform extraction imposes stringent restrictions on the pulsation of the current in the magnetic systems.[72] To establish the processes that make the main contributions to the beam modulation, a correlation method was developed to analyze the time structure of the beam, with apparatus to monitor the parameters.[77] It was found that the most stringent requirements are on the magnetic field of the accelerator. In order to meet these requirements, some studies in the power-supply system of the electromagnet were made,[78,79] and these helped to reduce the pulsations of the guiding magnetic field to the level 5×10^{-5}. The existing fluctuations of the parameters restrict the lower limit of the rate of passage through the resonance band, this being determined by the admissible level of beam density modulation during the extraction time. These factors put a lower limit on the intensity of a slowly extracted beam at a level $> 10^{11}$ protons/cycle. A rectangular intensity pulse of the extracted beam is formed by a beam feedback system,[80] which consists of a monitor of the extracted beam, an amplifier with regulated gain,[78] and blocks for controlling the currents of the quadrupole lens of the adjustment to resonance. The efficiency of elimination of the pulsations in the extracted beam by this system has a fundamental restriction with respect to the pulsation frequency due to the finite time of development of the resonance, which is about 1 msec. Therefore, the feedback circuit can effectively deal with pulsations only to frequencies around 100 Hz.

After excitation of the resonance, the particles are transferred into the gaps of the septum magnets (Fig. 24) with successively increasing thickness of the beam separating septum and, accordingly, increasing maximally possible field induction. This makes it possible to reduce the losses of the particles in the septum conductor. Deflection of the beam into the openings of the deflecting magnets is ensured by the creation of a local distortion of the beam orbit by switching on additional coils in the blocks Nos. 16 and 22. All the extraction magnets are fixed and placed outside the envelope of the beam circulating in the accelerator. To achieve more accurate adjustment and optimization of the beam tracks, the magnet DM-18 has remote-control adjustment in angle and radially. In the magnet DM-18 (Ref. 81), the beam is divided into two parts by a septum of thickness 0.5 mm, and the deflected part of the beam acquires in the magnetic field a deflection of about 0.435 mrad, which is necessary for deflection to the gap of the following magnet DM-20. The deflection acquired by the beam in the magnet DM-18 in the 20th straight section leads to a separation of the deflected beam from the circulating beam by a distance of about 8–9 mm. The extraction efficiency in this part of the track is determined largely by the losses of particles in the septum in DM-18 and by the effect of the stray magnetic field of the septum on the circulating beam. Figure 26 shows the simplified construction of the septum magnet DM-18. The magnetic circuit of the septum magnet is formed by three elements: the C-shaped part 2 of the magnetic circuit, the transition plate 13, and the pole tips 12, which are situated in the vacuum region. The C-shaped part is made of 10-mm steel plates in a packet of length 1280 mm. To transmit the magnetic flux within the vacuum chamber, which is made of stainless steel, the transition plate made of Kovar is used; it is connected by welding to the inner, 4, and outer, 8, chambers and forms a single vacuum region. The pole tips 12, made of single-piece plates, continue the magnetic circuit in the vacuum region. The excitation coil has a single winding and consists of the septum, 6, and reverse, 3, conductors, which are connected outside the vacuum region. The current barrier (septum conductor, support of septum) is made of a copper strip in thermal contact with the pole tips, which are heat-extraction radiators for it. The cooling is by a peripheral system of copper tubes soldered onto the

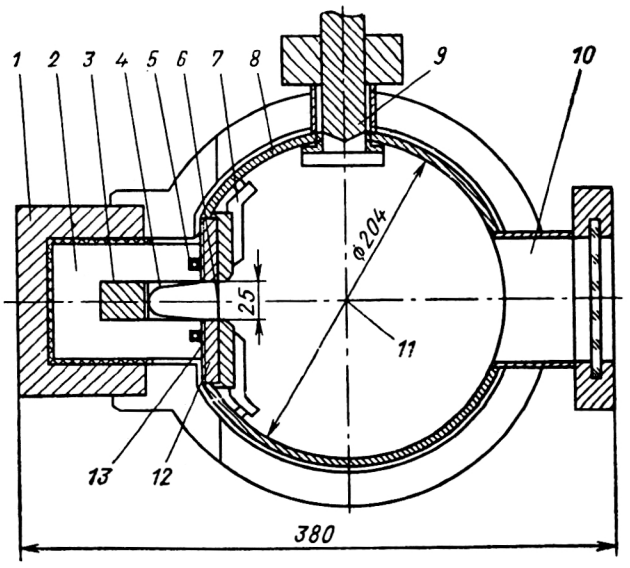

FIG. 26. Schematic diagram of transverse section of septum magnet DM-18 of the slow extraction system: 1) frame of magnetic circuit; 2) magnetic circuit; 3) return conductor of excitation coil; 4) internal vacuum chamber; 5) cooling tubes; 6) septum; 7) mechanical support device; 8) outer vacuum chamber; 9) unit of cooled current lead; 10) inspection window; 11) axis of vacuum chamber of accelerator; 12) pole tips; 13) transition plate.

transition plate, through which cooling water flows.

The magnets DM-20, 22, 26 have similar constructions[82] (Fig. 27) and differ in the number of windings in the coils: DM-20 has a coil with two windings, and the others have four windings. The septum conductor is made of copper conductors with internal channels for cooling water. The windings are connected at the end of the magnet, outside the vacuum region. The constructions of the magnets are very technological. The current connections outside the vacuum region and the water channels guarantee low gas release and high reliability of the construction. The main parameters of the magnets are given in Table II. The efficiency of proton extraction from the accelerator with magnets of such construction is about 85%, and the intensity of the extracted beam achieved by 1988 was about 5×10^{12} protons/cycle with modulation of the beam density in time of about 30–40%.

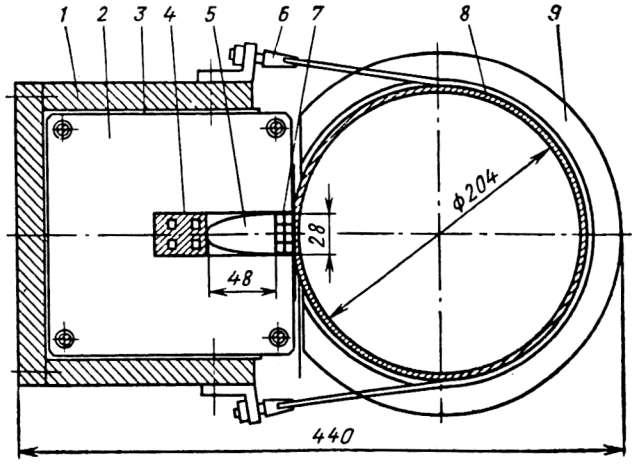

FIG. 27. Schematic diagram of transverse section of the septum magnet DM-26: 1) frame of magnetic circuit; 2) magnetic circuit; 3) insulation of magnetic circuit; 4) return conductors; 5) internal vacuum chamber; 6) support unit; 7) septum; 8) outer vacuum chamber; 9) rigidity ribs of chamber.

Nonresonant slow extraction of protons

As we have already noted, the intensity of the slowly extracted beam is bounded below in the IHEP accelerator by a value around 10^{11} protons/cycle. To extend the possibilities of experiments using the counter method and the formation of beams of lower intensity, use is made of extraction of part of the circulating beam in the accelerator by the selection of particles scattered by a target. This method is based on use of the slow extraction system for protons scattered elastically by an internal target of the accelerator[83,84] and extracted in the direction of channels Nos. 8 or 22. Particles passing through the target acquire an increment in the amplitude of the betatron oscillations, mainly through multiple Coulomb scattering and elastic nuclear scattering of beam particles by the target. The scattering angle depends on the material of the target, its length, and the number of passages of the beam through the target. With the existing arrangement of the septum magnets of the slow extraction system, the increment in the amplitude of the betatron oscillations acquired by the particles is not sufficient to deflect the beam into the openings of the deflecting magnets. To move the beam to the current barriers of the septums, a local perturbation of the beam orbit is created in the region of the septum magnets. The track of beam extraction from the accelerator is close to the ordinary track of the slowly extracted beam. The first investigations[83] showed that for extraction in the direction of channel No. 8 it is possible to use various internal targets, in particular, a target in the 35th magnetic block of the accelerator, which is used to generator secondary particles in channel No. 18. This makes possible simultaneous operation, in the cycle, of two facilities with one target. Besides this target, one can use targets in the 16th magnetic block, and also in the 17th and 18th straight sections. To deflect the particles into the openings of the deflecting magnets DM-18 and DM-20, a local distortion of the orbit is produced by switching on additional coils in the magnetic blocks Nos. 15, 16, 21, 22. For optimally chosen target parameters and values of the currents in the additional coils a phase space of the beam is formed that allows exploitation of a regime of the equipment in the extraction systems that is close to the usual regimes of resonant slow extraction, and this makes it easier to choose the forms of focusing of the beam in the head part of the channel and its formation on the external target.

With 6×10^{11} particles/cycle striking the target, the result was an extracted proton beam with intensity up to about 3×10^{10} particles/cycle and satisfactory beam inensity modulation at the level 30%.

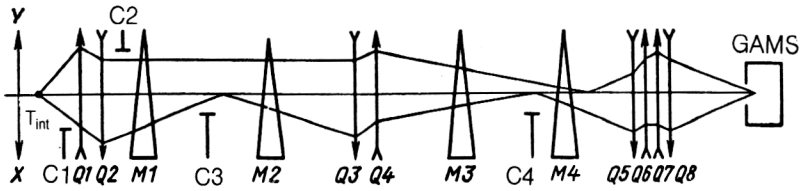

FIG. 28. Optical scheme of channel No. 4C to the facility GAMS: C are collimators; Q1–Q8 are magnetic lenses 20K200; M1 is an SP-12 magnet; M2 is an SP-7 magnet; M3 and M4 are SP-129 magnets; T_{int} is the internal target.

In the direction of channel No. 22, nonresonant slow extraction[84] was realized using thin targets[65] in the form of carbon tissue with thickness of about 0.3 mm. Two targets, placed in the magnetic blocks Nos. 24 and 27, are targets for the secondary-particle channels Nos. 2 and 4. Successive scattering of the beam by two thin targets allows the two main users of secondary beams (channels Nos. 2 and 4) and channel No. 22, in which the beam of protons elastically scattered from the targets for the FDOC facility is formed, to operate in their usual regime. The use of thin targets in such a regime made it possible to reduce appreciably the modulation of the beam intensity both in the secondary-particle channels (as was noted above) and in channel No. 22 with the extracted proton beams, where a beam of protons with intensity fluctuation of about 10% and duration of about 0.8 sec was obtained.

The development and use of the method of nonresonant slow extraction supplied the experimental facilities at the IHEP accelerator with extracted proton beams with energy 70 GeV extended over about 1 sec and in the intensity range 10^6–10^{10} protons/cycle with high uniformity in time.

5. CHANNELS FOR TRANSPORTING THE PARTICLES

Physics experiments with the IHEP accelerator are made possible by an extensive complex of channels that forms beams of particles with given parameters. Two groups of channels can be distinguished: internal-target secondary-particle channels, which are situated in building 1BV (see Fig. 1) and channels with proton beams extracted from the accelerator. The channels of the second group pass through building 1BV and transport the proton beams to the experimental facilities situated in buildings 2, 2a, PK-1, PK-2. The regime of operation of the accelerator with the channels is usually as follows. At the end of the acceleration cycle, at energy 70 GeV, there is a rapid extraction into channel No. 8; after 0.2–0.3 sec in the flat part of the magnetic cycle of the accelerator, at particle energy 70 GeV, slow extraction commences for use of the beam in one of the channels Nos. 21, 22, 23 with duration of about 1 sec; after a pause of about 0.2 sec, the remaining time of 0.9 sec on the plateau of the magnetic field is used for operation of the internal-target channels with simultaneous operation of up to three facilities.

Internal-target secondary-particle channels

This group includes channels Nos. 2, 4, 14, 18 and a channel of relativistic positronium.[85] Channel No. 6 has a simple configuration and is used for fault identification of the apparatus. A secondary-particle channel for the JINR BIS facility is under construction. To illustrate the method used to form a beam of secondary particles, we consider the optical scheme of channel No. 4C (Fig. 28), which transports the beam to the experimental facility GAMS. The negatively charged hadrons generated on a target in the magnetic block No. 27 are extracted by the magnetic field of the accelerator into the head part of the channel, where a flux of particles in the required interval of angles is taken from the total flux of particles by the vertical and horizontal collimators C1 and C2. The central region of

TABLE III. Characteristic parameters of beams in channels of secondary particles on internal targets of the accelerator.

Channel, facility	Particle species	Particle momentum GeV/c	Intensity at facility, particles/cycle	Momentum interval $\pm\Delta p/p$, %	Number of target
2A, MIS IHEP	h^- hadrons	40	2×10^6	1–2	24
2B, SIGMA	h^-	40	2×10^6	2	24
2C, KASKAD	e^-	28	5×10^5	3–4	24
2/14, PROZA	h^-	40	3×10^6	1–5	24
	e^-	26	6×10^4	1	24
4A, ISTRA	h^-	25	$\sim 10^7$	1–2	27
	e^-, e^+	10	2×10^5	1	27
4C, GAMS	h^-	38	$\sim 10^7$	1	27
	e^-	10	3×10^4	1	27
4D, VES	h^-	38	2×10^6	1	27
4E, MIS JINR	h^-	38	5×10^5	1	27
18, Giperon	h^+	10	10^8	2	35
	h^-	10	10^4	2	35
Pozitroniĭ	A_{2e}	0.8–2	0.02	-	35 $I = 2 \times 10^{11}$ protons/cycle

TABLE IV. Parameters of magneto-optical equipment of channels.

Equipment	Maximal current, kA	Induction, gradient	Opening of vacuum chamber ($r \times z$)	Mass, ton
Lens 20K200	3.5	13 T/m	Ø 180	8.9
Lens 10K200	1.1	20 T/m	Ø 80	2.2
Lens 20K100	3.5	13 T/m	Ø 180	4.6
Magnet SP-129	1.2	1.8 T	82×209	36.6
Magnet SP-032	1.76	1.6 T	144×300	34
Magnet SP-12	1.7	1.8 T	190×394	70
Magnet SP-7	2.43	1.8 T	190×394	96

the beam, bounded by the plates of the collimators, is occupied by the doublet of lenses Q1 and Q2, which are used for horizontal focusing to the center of the horizontal (so-called pulsed) collimator C3. The necessary dispersion with respect to the momentum in the region of this collimator is produced by the magnet M1. The opening of the plates of the collimator from the channel axis determines the momentum interval of the particles in the beam. The following magnet M2 deflects the beam in the direction of the experimental facility and partly compensates the momentum dispersion that has arisen. The doublet of lenses Q3 and Q4 fulfills the function of intermediate focusing of the beam. The collimator C4 is used to suppress the background particles that come within the beam halo. The final objective of the lenses Q5–Q8 is used to form the beam to the experimental facility with the required parameters. In contrast to the doublet of lenses, the triplet of lenses makes it possible to vary the spatial size and angular spread of the beam in a wider range.

Besides beams of hadrons, pure electron (positron) beams are also obtained in the channels.[86,87] The method of obtaining such beams is based on radiative decays of short-lived particles, mainly π^0 mesons, which are produced in a target by irradiating it with proton beams. The γ rays from the decay of the π^0 mesons produce electron–positron pairs as a result of conversion in the matter of a second target, called the converter. Charged hadrons are removed from the beam by means of an analyzing magnet in the section between the target and the converter. Using electron beams, one can also obtain beams of high-energy γ rays tagged with respect to the energy.[88]

A new direction in beam formation in this group of channels is the method of extracting the proton beam from the accelerator by channeling protons in a bent silicon single crystal placed in the vacuum chamber close to the periphery of the beam circulating in the accelerator. Such beams were obtained in channel No. 14 for the experimental facility PROZA. The proton beam was extracted by means of a single crystal bent through angle 80 mrad, and the obtained beam intensity was 4×10^6 protons/cycle.[89]

The characteristic parameters of beams realized in channels with 10^{12} protons/cycle directed onto the target are given in Table III, and the parameters of the magneto-optical equipment of the channels are given in Table IV. The characteristics of the beams are described in more detail in Refs. 90 and 91.

Channels for extracted proton beams

This group of channels is based on the systems of rapid and slow extraction of the proton beam from the accelerator. Both types of extraction are used in the case of channel No. 8. Channels Nos. 21 and 23 are branches of channel No. 8. The beam extracted slowly from the accelerator is transported through the head part of channel No. 8 by means of magnets in building 2, and the beam is deflected into the track of channel No. 21 or channel No. 23. Deflection into channel No. 21 is by means of pulsed magnets, and this permits simultaneous operation of channels Nos. 8 and 21 for rapid and slow extraction, respectively. The beam is deflected into channel No. 23 from the track of channel No. 8 by a permanent magnet. Simultaneous operation of channels Nos. 21 and 23 in the case of slow extraction has now been made possible by means of deflection of part of the beam by a bent single crystal.[92] The channels operate as follows. The magneto-optical systems are adjusted to transport the high-intensity beam to channel No. 23. A bent crystal is introduced into the beam, capturing the protons in the channeling regime and deflecting them through angles of 50–60 mrad; the capture efficiency is about 10^{-4}–10^{-5}. The low-intensity separated beam is directed along the track of channel No. 21. Further investigations determine the working range of intensities and parameters of the formed beams. Channel No. 22 is the high-intensity channel for slow extraction, the secondary beams for this being generated on an external target. Some characteristics of the beams in channels Nos. 8, 21, 22, and 23 are given in Table V.

The complex of systems of channel No. 8 is intended for the formation of a neutrino beam for the experimental facilities Neĭtrino, Neĭtrinnyĭ Detektor, and the bubble chamber SKAT. By the system for rapid extraction of the beam from the accelerator, a high-intensity proton beam is directed into channel No. 8 (Ref. 93), where it is focused by the magneto-optical system onto a target. The π and K mesons produced on the target are formed into a parallel beam by a special neutrino focusing device and, entering a vacuum tube with a length of about 120 m, decay, producing neutrino or antineutrino fluxes. The vacuum decay channel terminates with a massive steel filter, which shields the detectors from the hadronic and muonic backgrounds. The magneto-optical scheme of formation of the proton beam onto the target is shown in Fig. 29. The main problems that arise with the extraction and transporting of the intense beam are associated with the need to minimize the loss of particles,[73] which produce a radiation field along the channel track. The radiation along the channel track is monitored by a system of radiation monitors, and the losses of particles are measured by scintillation and Cherenkov counters set up along the vacuum ion guide of the channel. The currents in the lenses and magnets of the channel are monitored automatically. If the regimes violate the prescribed tolerances, the current monitoring system sends a signal that prevents beam extraction into the channel. If the established level of radiation is exceeded, extraction into the channel is also blocked by a system of radiation monitors.

TABLE V. Characteristic parameters of beams in channels of rapid and slow extraction.

Channel, facility	Intensity of protons extracted onto target (projected), particles/cycle	Secondary particles	Momentum, energy of secondary particles, GeV/c, GeV	Intensity of secondary particles, particles/cycle (at target 10^{12} protons/cycle)
8, Neĭtrinnyĭ Detektor, SKAT	3×10^{13}	ν_μ, $\overline{\nu_\mu}$	5–6	$\sim10^{-3}\frac{1}{m^2\cdot\text{proton}}$
21, SFINKS	2×10^{11}	p	70	10^6–10^{10}
	2×10^{12}	h^-	35	2×10^7
		h^+	35	3×10^8
23, Mechenye Neĭtrino	3×10^{13}	h^-	35	1.5×10^8
		h^+	35	2.5×10^9
22, FODS	10^{13}	h^+	40	2×10^9
	10^{13}	h^-	40	6×10^7
	10^{12}	e^-	30	10^6
	2×10^{11}	p	70	10^{10}

The target station of the neutrino channel is an extensive complex (Fig. 30). A thick concrete and metal shielding around the entrance to the target section must suppress radiation to levels that permit personnel to be present in the region behind the shield. The high level of induced radioactivity within this area imposes special requirements on the construction and reliability of the equipment in the target station. Transition from one part of the experiment to another requires replacement of equipment under conditions when the level of radiation 2–3 months after stopping of the channel is 2–5 rem/h. Repair of failed equipment 1–2 days after the channel has stopped operation requires work to be done under conditions of 10–50 rem/h. The main equipment of the target station is the target unit 9 and the objectives of the neutrino focusing device 3 and 6 (Fig. 30). The objectives[94] consist of pulsed focusing lenses, which are thin-wall paraboloids of revolution. Two paraboloids joined at their tips and forming an X-shaped construction form a lens. The electric busbars are fixed to the collars at the end of the wide end of the paraboloid. The objectives are powered through current leads (5) which pass through a labyrinth in the biological shield. The power-supply system provides currents in the lenses from 350 to 450 kA depending on the regime for a current pulse that lasts about 160 μsec. For remote disconnection of the current leads of the power-supply system and the busbars of the objectives there are fusible breakers 4 with tanks heated by electric coils. The electrical contact in the

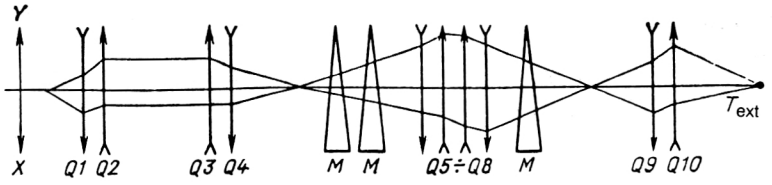

FIG. 29. Optical scheme of channel No. 8: Q1 and Q2 are magnetic lenses 7.5K150; Q3 and Q4 are lenses 10K200; Q5–Q10 are lenses 20K200; M are SP-129 magnets; T_{ext} is the external target.

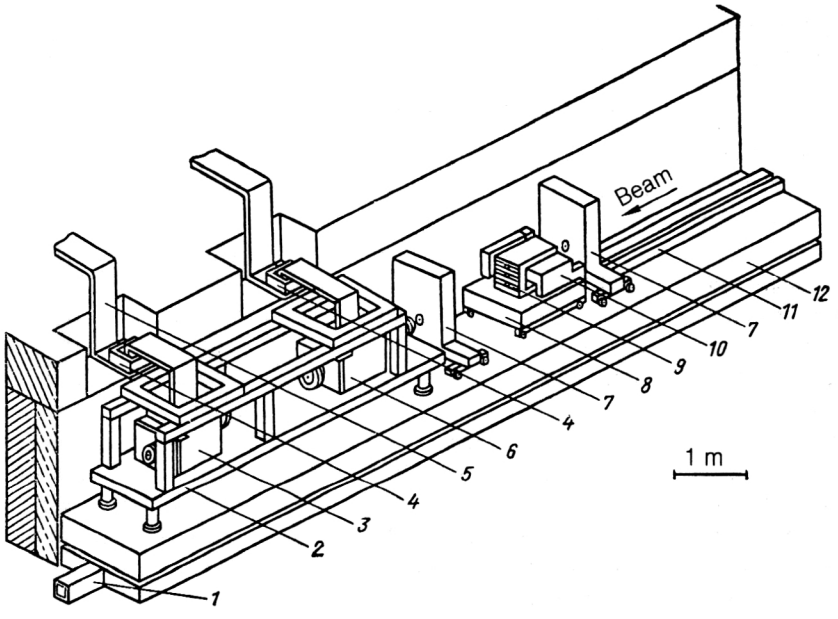

FIG. 30. Target station of neutrino channel No. 8 (first section of target station in configuration for formation of a broad-spectrum neutrino beam: 1) supply pipe for air cooling of objectives of neutrino-focusing device; 2) mounting of objectives Nos. 1 and 2; 3) objective No. 2; 4) fusible breaker; 5) current leads; 6) objective No. 1; 7) steel shielding screen; 8) target adjustment device; 9) target; 10) nozzle of system for air cooling of the target; 11) air pipes of the target cooling system; 12) general base.

tanks between the busbars of the current leads and the objectives is made by Wood's alloy. If the need arises, this alloy makes possible remote disconnection of the objectives and, with the upper shield of the entrance region removed, its evacuation by means of automatic capture, the presence of which is foreseen in the construction of the entire equipment. The system of the neutrino focusing device with three objectives provides intense neutrino fluxes with a wide spectrum at the detector.[94,95] Such a scheme has been realized since 1974 and forms neutrino and antineutrino beams with a wide spectrum and mean energy 5–6 GeV.

The parameters of the beams obtained in channel No. 8 are as follows. The intensity of the extracted beam achieved by 1988 was 1.3×10^{13} protons/cycle, and the beam diameter at the target was about 3–4 mm. The program of further development foresees the creation, in the channel, of beams of electron neutrinos and neutrinos with a narrow spectrum.[91]

Channel No. 21 was developed as a universal slow-extraction channel.[96] The program of investigations with the experimental facility SFINKS, which is situated in the channel, includes studies with not only proton beams but also beams of other secondary particles generated on an external target. At the present time, the experimental program can use the following channel regimes. Proton beams in the range of intensities 10^6–10^{10} protons/cycle are formed from the primary proton beam, which is extracted from the accelerator with intensity 5×10^{11} protons/cycle, at which a satisfactory beam density modulation is ensured. The beam can be collimated and reduced in intensity to 10^9–10^{10} particles/cycle. A proton beam with lower intensity 10^6–10^9 particles/cycle in the channel is obtained both by transporting protons that have been elastically scattered on an internal target[83] and extracted from the accelerator and by diffraction scattering of protons by an external target[96] of the channel itself. Another way of forming proton beams of moderate intensity is by means of a bent single crystal that traps a beam with an intensity of about 10^6–10^7 protons/cycle into the channeling regime.[97] The main part of the proton beam is absorbed in a collimator, and the beam deflected by the single crystal is transported by the following optics to the experimental facility. Beams of secondary particles are generated in a target in a special collimator. Up to 5×10^{12} protons/cycle can be directed onto the target. The channel makes it possible to form beams of positive particles with momentum 7–35 GeV/c and beams of negative particles with momentum 7–60 GeV/c.

Channel No. 23 (Ref. 98) forms beams for neutrino investigations with the experimental facility Mechenye Neĭtrino (tagged neutrinos). A slowly extracted beam of protons with projected intensity 3×10^{13} protons/cycle is transported through the head part of channel No. 8 and deflected by a permanent magnet into the track of channel No. 23. A doublet of quadrupole lenses focuses the beam onto a target in the section behind a thick biological shield. Secondary particles with momentum 5–35 GeV/c are trapped in a channel that forms a nearly parallel beam. In a vacuum tube with a length of about 65 m the kaons of the secondary beam decay into muon and electron neutrinos. Estimates show that at the projected intensity at the target of 3×10^{13} protons/cycle the kaon fluxes in the secondary beam will be at the level 2×10^9 particles/cycle. According to calculations, this will permit high-precision investigations with both muon and electron neutrinos with energy resolution of the events at the level 5–10%.[99]

Channel No. 22 was developed[91] to provide particle beams for two experimental facilities: FODS and, downbeam of it, SVD (a spectrometer with vertex detector in the form of the rapidly circulating bubble chamber). In the regime of operation with the facility FODS, a high-intensity hadron beam of 10^9 particles/cycle with momenta 10–60 Gev/c can be formed in the channel. Another regime of the channel makes it possible to form for the experimental facility FODS electron beams of intensity 10^5–10^6 with about 10^{12} protons/cycle being directed onto the target. The possibility is also foreseen of transporting 70-GeV protons scattered elastically by an internal target of the accelerator.

The formation of the beam for the SVD facility has certain special features. The load on the bubble chamber, which operates with frequency 20–30 Hz, must be at the level of 30–50 particles per activation. To dose the beam in the channel a beam intensity-modulation system is used. It is based on two powerful pulsed magnets, which are switched synchronously with the mechanism for expanding the bubble chamber. In front of the pulsed magnets there is a magnet with a constant field, which deflects the beam into an absorber. On activation of the first magnet, the beam is deflected into the track of the channel by a pulse with a steep leading edge. By means of a signal from a trigger in the bubble chamber that detects the particle flux, the power-supply system of the second magnet forms a current pulse in the coil and, the deflection obtained by the particles in the first pulsed magnet having been compensated in this manner, the beam is directed into the absorber. The pulse duration of the magnets is up to 80 μsec, and the current amplitude is about 4 kA. The magnets have single windings, and the field induction in the working gap is about 0.08 T. The particle dosing system together with the rapidly circulating bubble chamber entered the adjustment stage at the end of 1988. The working parameters of this complex will be adjusted in subsequent runs of the accelerator.

CONCLUSIONS

This review of the accelerator complex at the IHEP has been an attempt to give an overall picture of interrelated systems. This may have resulted in omissions and distortions in the description of individual systems because of the extensive nature and diversity of the material. The modernization of the U-70 accelerator complex in connection with the development of the accelerator and storage complex to energy 3000 GeV leads to changes in the systems of the existing operating accelerators and channels. In this connection, it is helpful at the completion of a definite stage in the development to sketch the contours of the results that have by now been achieved after a long period

of development of the U-70 complex. The data given here correspond to the actual characteristics of the systems at the beginning of 1989. It is probable that the description of some of the systems will have become outdated in view of the ongoing modernization by the time this paper is published. While recognizing this as inevitable, the author felt it was important to present as full a description as possible of the IHEP accelerator complex and to describe the technical decisions taken in developing the accelerator.

I thank Yu. M. Ado, A. A. Aseev, A. G. Afonin, V. P. Dan'shin, I. N. Dashkevich, V. G. Lapygin, O. P. Lebedev, V. A. Maisheev, A. V. Minchenko, É. A. Myaé, R. A. Razaev, O. N. Radin, V. B. Stepanov, and E. F. Troyanov, whose constructive remarks significantly improved the draft. I am also very grateful to V. A. Teplyakov and N. E. Tyurin for helpful advice and support of this work. I was assisted in preparing the draft by L. M. Komarova, L. Yu. Milichenko, and G. A. Nurusheva.

[1] V. V. Nizhegorodtsev, in *Proc. of the Fifth All-Union Symposium on Charged-Particle Accelerators*, Vol. 1 [in Russian] (Nauka, Moscow, 1977), p. 368.
[2] V. V. Nizhegorodtsev, "Inventor's Certificate No. 439232. Plasma ion source," Byull. Izobret. No. 27, 178 (1975).
[3] I. M. Kapchinskiĭ and V. A. Teplyakov, Prib. Tekh. Eksp. No. 2, 19 (1970).
[4] I. M. Kapchinskiĭ and V. A. Teplyakov, Prib. Tekh. Eksp. No. 4, 17 (1970).
[5] V. V. Vladimirskiĭ, Prib. Tekh. Eksp. No. 3, 35 (1956).
[6] V. A. Teplyakov, Prib. Tekh. Eksp. No. 6, 24 (1964).
[7] V. A. Teplyakov and V. B. Stepanov, Preprint 67-31-K [in Russian], IHEP, Serpukhov (1967).
[8] V. A. Teplyakov and V. B. Stepanov, Radiotekh. Electron. **13**, 1965 (1968).
[9] V. B. Stepanov and V. A. Teplyakov, Preprint 74-130 [in Russian], IHEP, Serpukhov (1974).
[10] A. L. Mints, in *Proc. of the First All-Union Symposium on Accelerators*, Vol. 1 [in Russian] (VINITI, Moscow, 1970), p. 67.
[11] A. P. Mal'tsev, S. M. Ermakov, and V. A. Teplyakov, At. Energ. **23**, 195 (1967).
[12] I. G. Mal'tsev and V. I. Nagaev, Preprint 85-134 [in Russian], IHEP, Serpukhov (1985).
[13] I. G. Mal'tsev and V. A. Teplyakov, Preprint 74-112 [in Russian], IHEP, Serpukhov (1974).
[14] E. V. Mazurov, I. G. Mal'tsev, A. B. Masaev *et al.*, in *Proc. of the Tenth All-Union Symposium on Accelerators*, Vol. 1 [in Russian] (Dubna, 1987), p. 197.
[15] I. G. Mal'tsev, in *Proc. of the Seventh All-Union Symposium on Accelerators*, Vol. 2 [in Russian] (Dubna, 1981), p. 30.
[16] I. G. Mal'tsev, Preprint 80-4 [in Russian], IHEP, Serpukhov (1980).
[17] Yu. M. Ado, V. I. Balbekov, A. A. Vasil'ev *et al.*, in *Proc. of the Second All-Union Symposium on Accelerators*, Vol. 1 [in Russian] (Nauka, Moscow, 1972), p. 47.
[18] É. A. Myaé, P. T. Pashkov, and A. V. Smirnov, Preprint 79-167 [in Russian], IHEP, Serpukhov (1979).
[19] V. I. Balbekov, K. P. Lomov, É. A. Myaé, and E. F. Troyanov, Preprint 82-76 [in Russian], IHEP, Serpukhov (1982).
[20] E. A. Aleev, V. L. Bruk, L. A. Glukhin *et al.*, in *Proc. of the Ninth All-Union Symposium on Accelerators*, Vol. 1 [in Russian] (Dubna, 1985), p. 14.
[21] V. L. Bruk, V. K. Vorob'ev, A. S. Gurevich *et al.*, in *Proc. of the Ninth All-Union Symposium on Accelerators*, Vol. 2 [in Russian] (Dubna, 1985), p. 25.
[22] O. A. Gusev, A. P. Lebedev, V. A. Titov *et al.*, in *Proc. of the Fourth All-Union Symposium on Accelerators*, Vol. 2 [in Russian] (Nauka, Moscow, 1975), p. 151.
[23] V. P. Goncharenko, O. A. Gusev, A. I. Konstantinov *et al.*, in *Proc. of the Tenth All-Union Symposium on Accelerators*, Vol. 1 [in Russian] (Dubna, 1987), p. 317.
[24] S. V. Vasin, G. F. Kuznetsov, É. A. Myaé *et al.*, in *Proc. of the Ninth All-Union Symposium on Accelerators*, Vol. 1 [in Russian] (Dubna, 1985), p. 391.
[25] V. L. Bruk, V. K. Vorob'ev, E. V. Klimenkov *et al.*, in *Proc. of the Ninth All-Union Symposium on Accelerators*, Vol. 2 [in Russian] (Dubna, 1985), p. 34.
[26] V. L. Bruk, V. K. Vorob'ev, L. A. Glukhikh *et al.*, in *Proc. of the Ninth All-Union Symposium on Accelerators*, Vol. 1 [in Russian] (Dubna, 1985), p. 156.
[27] É. A. Myaé, P. T. Pashkov, and A. V. Smirnov, Preprint 78-47 [in Russian], IHEP, Serpukhov (1978).
[28] A. D. Artemov, M. K. Bulgakov, I. N. Dashkevich, and M. P. Kalyamin, Preprint 89-65 [in Russian], IHEP, Serpukhov (1989).
[29] É. A. Myaé, V. I. Stolpovskiĭ, S. V. Schastlivtsev *et al.*, in *Proc. of the Tenth All-Union Symposium on Accelerators*, Vol. 2 [in Russian] (Dubna, 1987), p. 336.
[30] D. A. Demikhovskiĭ, A. M. Ivanov, G. F. Kuznetsov *et al.*, in *Proc. of the Eighth All-Union Symposium on Accelerators*, Vol. 1 [in Russian] (Dubna, 1983), p. 332.
[31] M. A. Anikeev, A. D. Artemov, B. S. Galkin *et al.*, in *Proc. of the Ninth All-Union Symposium on Accelerators*, Vol. 1 [in Russian] (Dubna, 1985), p. 395.
[32] V. P. Antipov, S. I. Balashin, S. L. Bogatyrev *et al.*, in *Proc. of the Ninth All-Union Symposium on Accelerators*, Vol. 1 [in Russian] (Dubna, 1985), p. 231.
[33] V. V. Vladimirskiĭ, E. G. Komar, A. L. Mints *et al.*, At. Energ. **4**, 31 (1956).
[34] E. G. Komar, I. F. Malyshev, I. A. Mozalevskiĭ *et al.*, in *Proc. of the First All-Union Symposium on Acceleration*, Vol. 1 [in Russian] (VINITI, Moscow, 1970), p. 164.
[35] V. D. Borisov, I. A. Mozalevskiĭ, N. A. Monoszon *et al.*, in *Proc. of the First All-Union Symposium on Acceleration*, Vol. 1 [in Russian] (VINITI, Moscow, 1970), p. 170.
[36] A. D. Ermolaev and M. F. Ovchinnikov, Preprint 83-165 [in Russian], IHEP, Serpukhov (1983).
[37] Yu. M. Ado, A. S. Gurevich, A. A. Kardash *et al.*, in *Proc. of the Tenth International Conference on Accelerators*, Vol. 2 [in Russian] (Serpukhov, 1977), p. 308.
[38] V. I. Balbekov and I. A. Shukeĭlo, Preprint 67-65 [in Russian], IHEP, Serpukhov (1967).
[39] Yu. M. Ado, V. I. Balbekov, K. P. Lomov, and É. A. Myaé, in *Proc. of the Second All-Union Symposium on Accelerators*, Vol. 2 [in Russian] (Nauka, Moscow, 1972), p. 17.
[40] V. L. Bruk, A. S. Gurevich, D. A. Demikhovskiĭ *et al.*, in *Proc. of the Fifth All-Union Symposium on Accelerators*, Vol. 2 [in Russian] (Nauka, Moscow, 1978), p. 9.
[41] V. L. Bruk, A. P. Lomov, N. G. Mamuchashvili *et al.*, in *Proc. of the Tenth International Conference on Accelerators*, Vol. 2 [in Russian] (Serpukhov, 1977), p. 364.
[42] S. N. Vasil'ev, G. I. Gusev, V. P. Dan'shin *et al.*, in *Proc. of the Eighth All-Union Symposium on Accelerators*, Vol. 2 [in Russian] (Dubna, 1983), p. 123.
[43] V. P. Dan'shin, V. I. Demyanchuk, A. A. Zhuravlev *et al.*, in *Proc. of the Sixth All-Union Symposium on Accelerators*, Vol. 2 [in Russian] (Dubna, 1979), p. 147.
[44] A. I. Bagin, Yu. S. Glukhov, E. V. Kornakov *et al.*, in *Proc. of the Second All-Union Symposium on Accelerators*, Vol. 1 [in Russian] (Nauka, Moscow, 1970), p. 159.
[45] B. A. Alekseev, V. I. Andreev, M. P. Vasil'ev *et al.*, in *Proc. of the Sixth All-Union Symposium on Accelerators*, Vol. 1 [in Russian] (Dubna, 1979), p. 216.
[46] A. M. Gudkov, B. M. Gutner, A. A. Zhuravlev *et al.*, in *Proc. of the Sixth All-Union Symposium on Accelerators*, Vol. 1 [in Russian] (Dubna, 1979), p. 307.
[47] A. M. Gudkov, I. P. Sulygin, and B. K. Shembel', Preprint 80-135 [in Russian], IHEP, Serpukhov (1980).
[48] A. D. Artemov, P. V. Bogdanov, M. A. Bulgakov *et al.*, Preprint 80-135 [in Russian], IHEP, Serpukhov (1980).
[49] S. S. Antonov, V. V. Zharenov, A. A. Kardash, and V. K. Perebeĭnos, Preprint 81-38 [in Russian], IHEP, Serpukhov (1981).
[50] O. P. Lebedev, Preprint 85-126 [in Russian], IHEP, Serpukhov (1985).
[51] V. L. Bruk, O. P. Lebedev, and V. M. Mokhov, Preprint 82-198 [in Russian], IHEP, Serpukhov (1982).
[52] V. P. Balbekov, K. F. Gertsev, and O. P. Lebedev, Preprint 84-23 [in

Russian], IHEP, Serpukhov (1984).
[53] Yu. M. Ado, A. I. Vershinin, O. P. Lebedev, and V. V. Polyakov, in *Proc. of the Tenth All-Union Symposium on Accelerators*, Vol. 1 [in Russian] (Dubna, 1987), p. 375.
[54] G. G. Gurov and A. Yu. Malovitskiĭ, Preprint 79-133 [in Russian], IHEP, Serpukhov (1978).
[55] G. G. Gurov, in *Proc. of the Seventh All-Union Symposium on Accelerators*, Vol. 1 [in Russian] (Dubna, 1981), p. 213.
[56] É. A. Myaé, in *Proc. of the Eighth All-Union Symposium on Accelerators*, Vol. 1 [in Russian] (Dubna, 1983), p. 231.
[57] Yu. Ado, M. N. Gorokhov, N. A. Ignashin *et al.*, Preprint 84-120 [in Russian], IHEP, Serpukhov (1984).
[58] V. I. Balbekov, K. F. Gertsev, L. I. Kopylov *et al.*, Preprint 85-129 [in Russian], IHEP, Serpukhov (1985).
[59] V. I. Balbekov, Preprint 85-128 [in Russian], IHEP, Serpukhov (1985).
[60] V. I. Balbekov, Preprint 86-73 [in Russian], IHEP, Serpukhov (1986).
[61] V. I. Balbekov, K. F. Gertsev, G. G. Gurov *et al.*, in *Proc. of the 13th International Conference on Accelerators*, Vol. 2 [in Russian] (Nauka, Moscow, 1987), p. 148.
[62] N. N. Dorokhin, A. Yu. Malovitskiĭ, É. A. Myaé, and P. T. Pashkov, Zh. Tekh. Fiz. **46**, 2577 (1976) [Sov. Phys. Tekh. Phys. **21**, 1521 (1976)].
[63] M. N. Gorokhov, A. A. Kardash, V. G. Shirokov *et al.*, Preprint 80-46 [in Russian], IHEP, Serpukhov (1980).
[64] V. I. Gridasov, A. A. Kardash, O. V. Kurnaev *et al.*, in *Proc. of the Seventh International Conference on Accelerators*, Vol. 1 [in Russian] (Erevan, 1970), p. 509.
[65] V. I. Gridasov, K. P. Myznikov, and V. N. Chepegin, At. Energ. **30**, 520 (1971).
[66] A. A. Aseev, V. N. Grishin, B. A. Zelenov *et al.*, Preprint 85-78 [in Russian], IHEP, Serpukhov (1985).
[67] V. I. Gridasov, K. P. Myznikov, and V. N. Chepegin, Preprint 73-78 [in Russian], IHEP, Serpukhov (1973).
[68] S. A. Belov, A. A. Kardash, V. A. Medvedev *et al.*, in *Proc. of the Sixth All-Union Symposium on Accelerators*, Vol. 1 [in Russian] (Dubna, 1979), p. 198.
[69] Yu. M. Ado, A. A. Aseev, A. A. Kardash *et al.*, Preprint 78-9 [in Russian], IHEP, Serpukhov (1988).
[70] K. P. Myznikov, in *Proc. of the Fifth All-Union Symposium on Accelerators*, Vol. 2 [in Russian] (Nauka, Moscow, 1978), p. 78.
[71] A. A. Aseev, A. G. Afonin, R. Bossart *et al.*, in *Proc. of the Third All-Union Symposium on Accelerators*, Vol. 2 [in Russian] (Nauka, Moscow, 1973), p. 160.
[72] V. V. Komarov, O. V. Kurnaev, Yu. V. Kuyanov *et al.*, in *Proc. of the Eighth All-Union Symposium on Accelerators*, Vol. 1 [in Russian] (Dubna, 1983), p. 336.
[73] A. G. Afonin, G. I. Britvich, N. A. Galyaev *et al.*, Preprint 86-3 [in Russian], IHEP, Serpukhov (1986).
[74] K. P. Myznikov, V. I. Gridasov, O. V. Kurnaev *et al.*, in *Proc. of the Seventh All-Union Symposium on Accelerators*, Vol. 1 [in Russian] (Erevan, 1970), p. 480.
[75] K. P. Myznikov, V. M. Tatarenko, and Yu. S. Fedotov, Preprint 70-51 [in Russian], IHEP, Serpukhov (1970).
[76] V. K. Vorob'ev, A. V. Levin, L. L. Moĭzhes *et al.*, in *Proc. of the Tenth All-Union Symposium on Accelerators*, Vol. 2 [in Russian] (Serpukhov, 1977), p. 157.
[77] V. V. Komarov, A. A. Matyushin, K. P. Myznikov *et al.*, in *Proc. of the Fifth All-Union Symposium on Accelerators*, Vol. 2 [in Russian] (Nauka, Moscow, 1978), p. 92.
[78] B. V. Kaz'min, L. L. Moĭzhes, É. V. Polyakov *et al.*, Prib. Tekh. Eksp. No. 1, 17 (1977).
[79] V. K. Vorob'ev and L. L. Moĭzhes, Prib. Tekh. Eksp. No. 2, 32 (1977).
[80] A. I. Drozhdin, B. A. Zelenov, A. A. Kardash *et al.*, in *Proc. of the Fifth All-Union Symposium on Accelerators*, Vol. 2 [in Russian] (Nauka, Moscow, 1978), p. 88.
[81] Yu. M. Ado and É. A. Lyudmirskiĭ, Preprint 87-30 [in Russian], IHEP, Serpukhov (1987).
[82] Yu. M. Ado, A. G. Daĭkovskiĭ, S. Yu. Ershov, and É. A. Lyudmirskiĭ, Preprint 87-37 [in Russian], IHEP, Serpukhov (1987).
[83] Yu. M. Ado, A. A. Aseev, V. N. Grishin *et al.*, Preprint 85-23 [in Russian], IHEP, Serpukhov (1985).
[84] A. A. Aseev, N. A. Galyaev, V. N. Zapol'skiĭ *et al.*, Preprint 89-78 [in Russian], IHEP, Serpukhov (1989).
[85] Yu. M. Ado, A. G. Afonin, A. A. Zhuravlev *et al.*, in *Proc. of the Tenth All-Union Symposium on Accelerators*, Vol. 1 [in Russian] (Serpukhov, 1977), p. 44.
[86] S. S. Gershteĭn, A. V. Samoĭlov, Yu. M. Sapunov *et al.*, Preprint 72-93 [in Russian], IHEP, Serpukhov (1972).
[87] M. D. Bavizhev, N. K. Bulgakov, P. Voĭtkovska *et al.*, Preprint 82-74 [in Russian], IHEP, Serpukhov (1982).
[88] A. S. Belousov, B. B. Govorkov, V. A. Maisheev *et al.*, "Electron beams of proton accelerators and investigations of electromagnetic processes," Tr. Fiz. Inst. Akad. Nauk SSSR **143**, 34 (1983).
[89] A. A. Aseev, M. D. Bavizhev, I. V. Bakula *et al.*, Preprint 89-57 [in Russian], IHEP, Serpukhov (1989).
[90] Yu. M. Ado, A. G. Afonin, N. A. Galyaev *et al.*, Preprint 85-182 [in Russian], IHEP, Serpukhov (1985).
[91] Yu. M. Ado, A. G. Afonin, N. A. Galyaev *et al.*, in *Proc. of the Tenth All-Union Symposium on Accelerators*, Vol. 2 [in Russian] (Dubna, 1987), p. 346.
[92] M. D. Bavizhev, N. A. Galyaev, V. N. Gres' *et al.*, Preprint 89-77 [in Russian], IHEP, Serpukhov (1989).
[93] D. G. Baratov, M. M. Zaĭtsev, V. I. Kotov *et al.*, Preprint 76-86 [in Russian], IHEP, Serpukhov (1976).
[94] D. G. Baratov, N. Z. Bikbulatov, V. V. Vasil'ev *et al.*, Preprint 76-87 [in Russian], IHEP, Serpukhov (1976).
[95] V. N. Voronov, I. A. Danil'chenko, R. A. Rzaev, and A. V. Samoĭlov, Preprint 70-93 [in Russian], IHEP, Serpukhov (1970).
[96] A. A. Batalov, I. A. Vetlitskiĭ, N. A. Galyaev *et al.*, Preprint 87-116 [in Russian], IHEP, Serpukhov (1987).
[97] M. D. Bavizhev, A. A. Batalov, N. A. Galyaev *et al.*, Preprint 87-148 [in Russian], IHEP, Serpukhov (1987).
[98] M. V. Akopyan, A. A. Batalov, A. P. Bugorskiĭ, Preprint 86-129 [in Russian], IHEP, Serpukhov (1986).
[99] A. A. Boikov, S. P. Denison, A. V. Erokhin *et al.*, Preprint 80-156 [in English], IHEP, Serpukhov (1980).

Translated by Julian B. Barbour